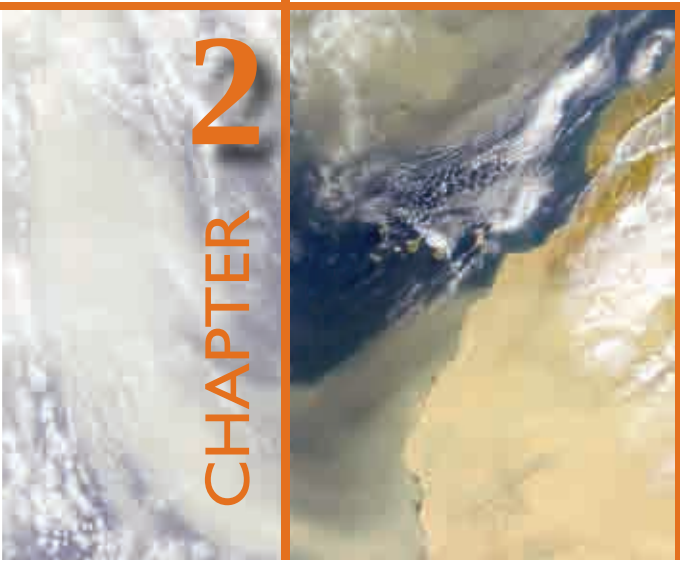

CHAPTER 2

Remote Sensing and *In Situ* Measurements of Aerosol Properties, Burdens, and Radiative Forcing

Lead Authors: Hongbin Yu, NASA GSFC/UMBC; Patricia K. Quinn, NOAA PMEL; Graham Feingold, NOAA ESRL; Lorraine A. Remer, NASA GSFC; Ralph A. Kahn, NASA GSFC
Contributing Authors: Mian Chin, NASA GSFC; Stephen E. Schwartz, DOE BNL

2.1. Introduction

As discussed in Chapter 1, much of the challenge in quantifying aerosol direct radiative forcing (DRF) and aerosol-cloud interactions arises from large spatial and temporal heterogeneity of aerosol concentrations, compositions, and sizes, which requires an integrated approach that effectively combines measurements and model simulations. Measurements, both *in situ* and remote sensing, play essential roles in this approach by providing data with sufficient accuracy for validating and effectively constraining model simulations. For example, to achieve an accuracy of 1 W m^{-2} for the instantaneous, top-of-atmosphere (TOA) aerosol DRF under cloud free conditions, the accuracy for measuring aerosol optical depth (AOD) should be within 0.01 and 0.02 for mid-visible wavelength, and that for single-scattering albedo (SSA) should be constrained to about 0.02 over land (Chapter 1, Table 1.2). The measurement requirements would be much tighter in order to achieve the same forcing accuracy at the surface. Quantifying anthropogenic component of DRF and aerosol indirect radiative forcing would impose additional accuracy requirements on measurements of aerosol chemical composition and microphysical properties (e.g., size distribution) that are needed to attribute material to sources or source type.

Over the past decade and since the Intergovermental Panel on Climate Change (IPCC) Third Assessment Report (TAR) (IPCC 2001) in particular, a great deal of effort has gone into improving measurement data sets (as summarized in Yu et al., 2006; Bates et al., 2006; Kahn et al., 2004). Principal efforts have been:

- Development and implementation of new and enhanced satellite-borne sensors examining aerosol effects on atmospheric radiation;
- Execution of focused field experiments examining aerosol processes and properties in various aerosol regimes around the globe;
- Establishment and enhancement of ground-based networks measuring aerosol properties and radiative forcing; and
- Development and deployment of new and enhanced instrumentation, importantly aerosol mass spectrometers examining size dependent composition and several methods for measuring aerosol SSA.

These efforts have made it feasible to shift the estimates of aerosol radiative forcing increasingly from largely model-based as in IPCC TAR to measurement-based as in the IPCC Fourth Assessment Report (AR4) (IPCC 2007). Satellite measurements that are evaluated, supplemented, and constrained by ground-based remote sensing measurements and *in situ* measurements from focused field campaigns, provide the basis for the regional- to global-scale assessments. Chemistry and transport models (CTMs) are used to interpolate and supplement the data in regions and under conditions where observational data are not available or to assimilate high-quality data from various observations to constrain and thereby improve

model simulations of aerosol impacts. These developments have played an important role in advancing the scientific understanding of aerosol direct and indirect radiative forcing as documented in the IPCC AR4 (IPCC, 2007).

The goals of this chapter are to:

- provide an overview of current aerosol measurement capabilities and limitations;
- describe the concept of synergies between different types of measurements and models;
- assess estimates of aerosol direct and indirect radiative forcing from different observational approaches; and
- discuss outstanding issues to which measurements can contribute.

The synthesis and assessment in this chapter lays groundwork needed to develop a future research strategy for understanding and quantifying aerosol-climate interactions.

Satellite remote sensing is the only means of characterizing the large spatial and temporal heterogeneities of aerosol distributions.

2.2. Overview of Aerosol Measurement Capabilities

2.2.1. Satellite Remote Sensing

A measurement-based characterization of aerosols on a global scale can be realized only through satellite remote sensing, which is the only means of characterizing the large spatial and temporal heterogeneities of aerosol distributions. Monitoring aerosols from space has been performed for over two decades and is planned for the coming decade with enhanced capabilities (King et al., 1999; Foster et al., 2007; Lee et al., 2006; Mishchenko et al., 2007b). Table 2.1 summarizes major satellite measurements currently available for the tropospheric aerosol characterization and radiative forcing research.

Early aerosol monitoring from space relied on sensors that were designed for other purposes. The Advanced Very High Resolution Radiometer (AVHRR), intended as a cloud and surface monitoring instrument, provides radiance observations in the visible and near infrared wavelengths that are sensitive to aerosol properties over the ocean (Husar et al., 1997; Mishchenko et al., 1999). Originally intended for ozone monitoring, the ultraviolet (UV) channels used for the Total Ozone Mapping Spectrometer (TOMS) are sensitive to aerosol UV absorption with little surface interferences, even over land (Torres et al., 1998). This UV-technique makes TOMS suitable for monitoring biomass burning smoke and dust, though with limited sensitivity near the surface (Herman et al., 1997) and for retrieving aerosol single-scattering albedo from space (Torres et al., 2005). (A new sensor, the Ozone Monitoring Instrument (OMI) aboard Aura, has improved on such UV-technique advantages, providing higher spatial resolution and more spectral channels, see Veihelmann et al., 2007). Such historical sensors have provided multi-decadal climatology of aerosol optical depth that has significantly advanced the understanding of aerosol distributions and long-term variability (e.g., Geogdzhayev et al., 2002; Torres et al., 2002; Massie et al., 2004; Mishchenko et al., 2007a; Mishchenko and Geogdzhayev, 2007; Zhao et al., 2008a).

Over the past decade, satellite aerosol retrievals have become increasingly sophisticated. Now, satellites measure the angular dependence of radiance and polarization at multiple wavelengths from UV through the infrared (IR) at fine spatial resolution. From these observations, retrieved aerosol products include not only optical depth at one wavelength, but also spectral optical depth and some information about particle size over both ocean and land, as well as more direct measurements of polarization and phase function. In addition, cloud screening is much more robust than before and onboard calibration is now widely available. Examples of such new and enhanced sensors include the MODerate resolution Imaging Spectroradiometer (MODIS, see Box 2.1), the Multi-angle Imaging SpectroRadiometer (MISR, see Box 2.2), Polarization and Directionality of the Earth's Reflectance (POLDER, see Box 2.3), and OMI, among others. The accuracy for AOD measurement from these sensors is about 0.05 or 20% of AOD (Remer et al., 2005; Kahn et al., 2005a) and somewhat better over dark water, but that for aerosol microphysical properties, which is useful for distinguishing aerosol air mass types, is generally low. The Clouds and the Earth's Radiant Energy System (CERES, see Box 2.4) measures broadband solar and terrestrial radiances. The CERES radiation measurements in combination with satellite retrievals of aerosol optical depth can be used to determine aerosol direct radiative forcing.

Table 2.1. Summary of major satellite measurements currently available for the tropospheric aerosol characterization and radiative forcing research.

Category	Properties	Sensor/platform	Parameters	Spatial coverage	Temporal coverage
Column-integrated	Loading	AVHRR/NOAA-series	optical depth	~daily coverage of global ocean	1981-present
		TOMS/Nimbus, ADEOS1, EP		~daily coverage of global land and ocean	1979-2001
		POLDER-1, -2, PARASOL			1997-present
		MODIS/Terra, Aqua			2000-present (Terra) 2002-present (Aqua)
		MISR/Terra		~weekly coverage of global land and ocean, including bright desert and nadir sun-glint	2000-present
		OMI/Aura		~daily coverage of global land and ocean	2005-present
	Size, shape	AVHRR/NOAA-series	Ångström exponent	global ocean	1981-present
		POLDER-1, -2, PARASOL	fine-mode fraction, Ångström exponent, non-spherical fraction	global land+ocean	1997-present
		MODIS/Terra, Aqua	fine-mode fraction	global land+ocean (better quality over ocean)	2000-present (Terra) 2002-present (Aqua)
			Ångström exponent		
			effective radius	global ocean	
			asymmetry factor		
		MISR/Terra	Ångström exponent, small, medium, large fractions, non-spherical fraction	global land+ocean	2000-present
	Absorption	TOMS/Nimbus, ADEOS1, EP	absorbing aerosol index, single-scattering albedo, absorbing optical depth	global land+ocean	1979-2001
		OMI/Aura			2005-present
		MISR/Terra	single-scattering albedo (2-4 bins)		2000-present
Vertical-resolved	Loading, size, and shape	GLAS/ICESat	extinction/backscatter	global land+ocean, 16-day repeating cycle, single-nadir measurement	2003-present (~3months/year)
		CALIOP/CALIPSO	extinction/backscatter, color ratio, depolarization ratio		2006-present

Box 2.1: MODerate resolution Imaging Spectroradiometer

MODIS performs near global daily observations of atmospheric aerosols. Seven of 36 channels (between 0.47 and 2.13 μm) are used to retrieve aerosol properties over cloud and surface-screened areas (Martins et al., 2002; Li et al., 2004). Over vegetated land, MODIS retrieves aerosol optical depth at three visible channels with high accuracy of $\pm 0.05 \pm 0.2\tau$ (Kaufman et al., 1997; Chu et al., 2002; Remer et al., 2005; Levy et al., 2007b). Most recently a deep-blue algorithm (Hsu et al., 2004) has been implemented to retrieve aerosols over bright deserts on an operational basis, with an estimated accuracy of 20-30%. Because of the greater simplicity of the ocean surface, MODIS has the unique capability of retrieving not only aerosol optical depth with greater accuracy, i.e., $\pm 0.03 \pm 0.05\tau$ (Tanré et al., 1997; Remer et al., 2002; 2005; 2008), but also quantitative aerosol size parameters (e.g., effective radius, fine-mode fraction of AOD) (Kaufman et al., 2002a; Remer et al., 2005; Kleidman et al., 2005). The fine-mode fraction has been used as a tool for separating anthropogenic aerosol from natural ones and estimating the anthropogenic aerosol direct climate forcing (Kaufman et al., 2005a). Figure 2.1 shows composites of MODIS AOD and fine-mode fraction that illustrate seasonal and geographical variations of aerosol types. Clearly seen from the figure is heavy pollution over East Asia in both months, biomass burning smoke over South Africa, South America, and Southeast Asia in August, heavy dust storms over North Atlantic in both months and over Arabian Sea in August, and a mixture of dust and pollution plume swept across North Pacific in April.

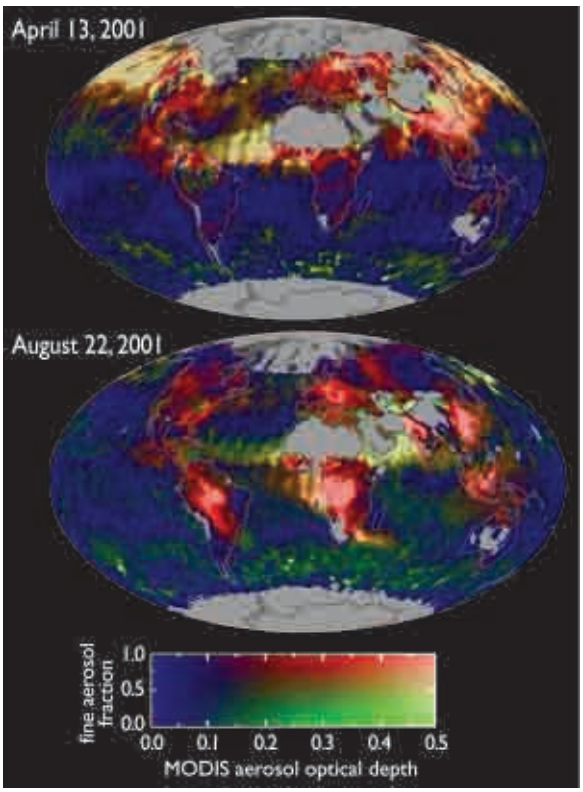

Figure 2.1. A composite of MODIS/Terra observed aerosol optical depth (at 550 nm, green light near the peak of human vision) and fine-mode fraction that shows spatial and seasonal variations of aerosol types. Industrial pollution and biomass burning aerosols are predominately small particles (shown as red), whereas mineral dust and sea salt consist primarily of large particles (shown as green). Bright red and bright green indicate heavy pollution and dust plumes, respectively (adapted from Chin et al., 2007; original figure from Yoram Kaufman and Reto Stöckli).

Complementary to these passive sensors, active remote sensing from space is also now possible and ongoing (see Box 2.5). Both the Geoscience Laser Altimeter System (GLAS) and the Cloud and Aerosol Lidar with Orthogonal Polarization (CALIOP) are collecting essential information about aerosol vertical distributions. Furthermore, the constellation of six afternoon-overpass spacecrafts (as illustrated in Figure 2.5), the so-called A-Train (Stephens et al., 2002) makes it possible for the first time to conduct near simultaneous (within 15-minutes) measurements of aerosols, clouds, and radiative fluxes in multiple dimensions with sensors in complementary capabilities.

The improved accuracy of aerosol products (mainly AOD) from these new-generation sensors, together with improvements in characterizing the earth's surface and clouds, can help reduce the uncertainties associated with estimating the aerosol direct radiative forcing (Yu et al., 2006; and references therein). The retrieved aerosol microphysical properties, such as size, absorption, and non-spherical fraction can help distinguish anthropogenic

aerosols from natural aerosols and hence help assess the anthropogenic component of aerosol direct radiative forcing (Kaufman et al., 2005a; Bellouin et al., 2005, 2008; Christopher et al., 2006; Yu et al., 2006, 2008). However, to infer aerosol number concentrations and examine indirect aerosol radiative effects from space, significant efforts are needed to measure aerosol size distribution with much improved accuracy, characterize aerosol type, account for impacts of water uptake on aerosol optical depth, and determine the fraction of aerosols that is at the level of the clouds (Kapustin et al., 2006; Rosenfeld, 2006). In addition, satellite remote sensing is not sensitive to particles much smaller than 0.1 micrometer in diameter, which comprise of a significant fraction of those that serve as cloud condensation nuclei.

Finally, algorithms are being developed to retrieve aerosol absorption or SSA from satellite observations (e.g., Kaufman et al., 2002b; Torres et al., 2005). The NASA Glory mission, scheduled to launch in 2009 and to be added to the A-Train, will deploy a multi-angle, multi-spectral polarimeter to determine the global distribution of aerosol and clouds. It will also be able to infer microphysical property information, from which aerosol type (e.g., marine, dust, pollution, etc.) can be inferred for improving quantification of the aerosol direct and indirect forcing on climate (Mishchenko et al., 2007b).

In summary, major advances have been made in both passive and active aerosol remote sensing from space in the past decade, providing better coverage, spatial resolution, retrieved AOD accuracy, and particle property information. However, AOD accuracy is still much poorer than that from surface-based sun photometers (0.01 to 0.02), even over vegetated land and dark water where retrievals are most reliable. Although there is some hope of approaching this level of uncertainty with a new generation of satellite instruments, the satellite retrievals entail additional sensitivities to aerosol and surface scattering properties. It seems unlikely that satellite remote sensing could exceed the sun photometer accuracy without introducing some

Major advances have been made in both passive and active aerosol remote sensing from space in the past decade, providing better coverage, spatial resolution, retrieved AOD accuracy, and particle property information.

Box 2.2: Multi-angle Imaging SpectroRadiometer

MISR, aboard the sun-synchronous, polar orbiting satellite Terra, measures upwelling solar radiance in four visible-near-IR spectral bands and at nine view angles spread out in the forward and aft directions along the flight path (Diner et al., 2002). It acquires global coverage about once per week. A wide range of along-track view angles makes it feasible to more accurately evaluate the surface contribution to the TOA radiances and hence retrieve aerosols over both ocean and land surfaces, including bright desert and sunglint regions (Diner et al., 1998; Martonchik et al., 1998a; 2002; Kahn et al., 2005a). MISR AODs are within 20% or ±0.05 of coincident AERONET measurements (Kahn et al., 2005a; Abdou et al., 2005). The MISR multi-angle data also sample scattering angles ranging from about 60° to 160° in midlatitudes, yielding information about particle size (Kahn et al., 1998; 2001; 2005a; Chen et al., 2008) and shape (Kalashnikova and Kahn, 2006). The aggregate of aerosol microphysical properties can be used to assess aerosol airmass type, a more robust characterization of MISR-retrieved particle property information than individual attributes. MISR also retrieves plume height in the vicinity of wildfire, volcano, and mineral dust aerosol sources, where the plumes have discernable spatial contrast in the multi-angle imagery (Kahn et al., 2007a). Figure 2.2 is an example that illustrates MISR's ability to characterize the load, optical properties, and stereo height of near-source fire plumes.

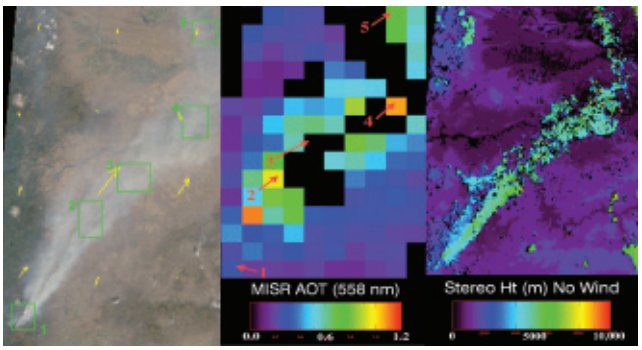

Figure 2.2. Oregon fire on September 4, 2003 as observed by MISR: (a) MISR nadir view of the fire plume, with five patch locations numbered and wind-vectors superposed in yellow; (b) MISR aerosol optical depth at 558 nm; and (c) MISR stereo height without wind correction for the same region (taken from Kahn et al., 2007a).

Box 2.3: POLarization and Directionality of the Earth's Reflectance

POLDER is a unique aerosol sensor that consists of wide field-of-view imaging spectro-radiometer capable of measuring multi-spectral, multi-directional, and polarized radiances (Deuzé et al., 2001). The observed radiances can be exploited to better separate the atmospheric contribution from the surface contribution over both land and ocean. POLDER -1 and -2 flew onboard the ADEOS (Advanced Earth Observing Satellite) from November 1996 to June 1997 and April to October of 2003, respectively. A similar POLDER instrument flies on the PARASOL satellite that was launched in December 2004.

Figure 2.3 shows global horizontal patterns of AOD and Ångström exponent over the oceans derived from the POLDER instrument for June 1997. The oceanic AOD map (Figure 2.3.a) reveals near-coastal plumes of high AOD, which decrease with distance from the coast. This pattern arises from aerosol emissions from the continents, followed by atmospheric dispersion, transformation, and removal in the downwind direction. In large-scale flow fields, such as the trade winds, these continental plumes persist over several thousand kilometers. The Ångström exponent shown in Figure 2.3.b exhibits a very different pattern from that of the aerosol optical depth; specifically, it exhibits high values downwind of industrialized regions and regions of biomass burning, indicative of small particles arising from direct emissions from combustion sources and/or gas-to-particle conversion, and low values associated with large particles in plumes of soil dust from deserts and in sea salt aerosols.

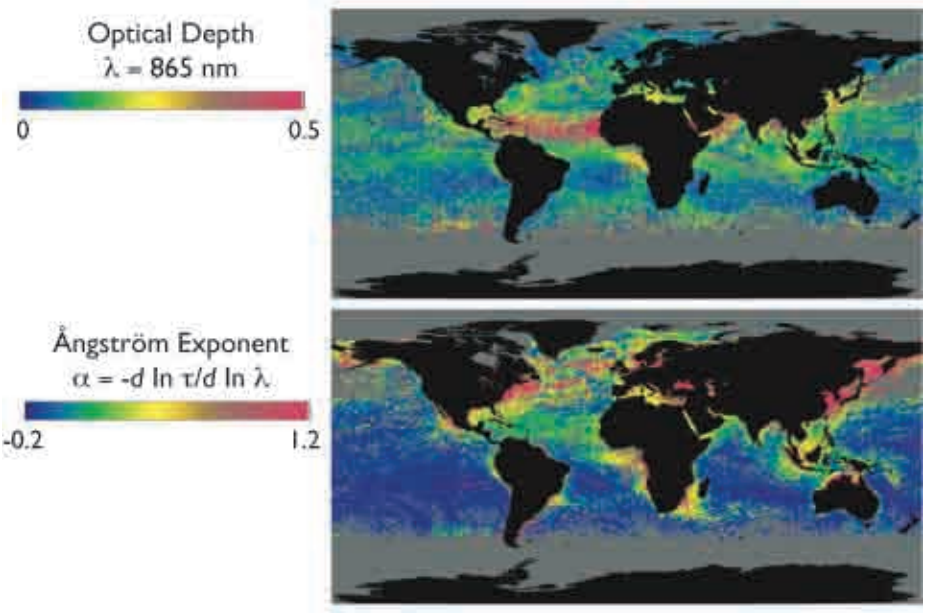

Figure 2.3. Global maps at 18 km resolution showing monthly average (a) AOD at 865 nm and (b) Ångström exponent of AOD over water surfaces only for June, 1997, derived from radiance measurements by the POLDER. Reproduced with permission of Laboratoire d'Optique Atmospherique (LOA), Lille, FR; Laboratoire des Sciences du Climat et de l'Environnement (LSCE), Gif sur Yvette, FR; Centre National d'etudes Spatiales (CNES), Toulouse, FR; and NAtional Space Development Agency (NASDA), Japan.

as-yet-unspecified new technology. Space-based lidars are for the first time providing global constraints on aerosol vertical distribution, and multi-angle imaging is supplementing this with maps of plume injection height in aerosol source regions. Major advances have also been made during the past decade in distinguishing aerosol types from space, and the data are now useful for validating aerosol transport model simulations of aerosol air mass type distributions and transports, particularly over dark water. But particle size, shape, and especially SSA information has large uncertainty; improvements will be needed to better distinguish anthropogenic from natural aerosols using space-based retrievals. The particle microphysical property detail required to assess aerosol radiative forcing will come largely from targeted *in situ* and surface remote sensing measurements, at least for the near-future, although estimates of measurement-based aerosol RF can be made from judicious use of the satellite data with relaxed requirements for characterizing aerosol microphysical properties.

2.2.2. Focused Field Campaigns

Over the past two decades, numerous focused field campaigns have examined the physical, chemical, and optical properties and radiative forcing of aerosols in a variety of aerosol regimes around the world, as listed in Table 2.2. These campaigns, which have been designed with aerosol characterization as the main goal or as one of the major themes in more interdisciplinary studies, were conducted mainly over or downwind of known continental aerosol source regions, but in some instances in low-aerosol regimes, for contrast. During each of these comprehensive campaigns, aerosols were studied in great detail, using combinations of *in situ* and remote sensing observations of physical and chemical properties from various platforms (e.g., aircraft, ships, satellites, and ground-based stations) and numerical modeling. In spite of their relatively short duration, these field studies have acquired comprehensive data sets of regional aerosol properties that have been used to understand the properties and evolution of aerosols within the atmosphere and to improve the climatology of aerosol microphysical properties used in satellite retrieval algorithms and CTMs.

2.2.3. Ground-based In situ Measurement Networks

Major US-operated surface *in situ* and remote sensing networks for tropospheric aerosol characterization and climate forcing research are listed in Table 2.3. These surface *in situ* stations provide information about long-term changes and trends in aerosol concentrations and properties, the influence of regional sources on aerosol properties, climatologies of aerosol radiative properties, and data for testing models (e.g., Quinn et al., 2000; Quinn et al., 2002; Delene and Ogren, 2002; Sheridan and Ogren, 1999; Fiebig and Ogren, 2006; Bates et al., 2006; Quinn et al., 2007) and satellite aerosol retrievals. The NOAA Earth System Research Laboratory (ESRL) aerosol monitoring network consists of baseline, regional, and mobile stations. These near-surface measurements include submicrometer and sub-10 micrometer scattering and absorption coefficients from which the extinction coefficient and single-scattering albedo can be derived. Additional measurements include particle concentration and, at selected sites, CCN concentration, the hygroscopic growth factor, and chemical composition.

Several of the stations, which are located across North America and world-wide, are in regions where recent focused field campaigns have been conducted. The measurement protocols at the stations are similar to those used during the field campaigns. Hence, the station data are directly comparable to the field campaign data so that they provide a longer-term measure of mean aerosol properties and their variability, as well as a context for the shorter-duration measurements of the field campaigns.

Box 2.4: Clouds and the Earth's Radiant Energy System

CERES measures broadband solar and terrestrial radiances at three channels with a large footprint (e.g., 20 km for CERES/Terra) (Wielicki et al., 1996). It is collocated with MODIS and MISR aboard Terra and with MODIS on Aqua. The observed radiances are converted to TOA irradiances or fluxes using the Angular Distribution Models (ADMs) that are functions of viewing angle, sun angle, and scene type (Loeb and Kato, 2002; Zhang et al., 2005a; Loeb et al., 2005). Such estimates of TOA solar flux in clear-sky conditions can be compared to the expected flux for an aerosol-free atmosphere, in conjunction with measurements of aerosol optical depth from other sensors (e.g., MODIS and MISR) to derive the aerosol direct radiative forcing (Loeb and Manalo-Smith, 2005; Zhang and Christopher, 2003; Zhang et al., 2005b; Christopher et al., 2006; Patadia et al., 2008). The derived instantaneous value is then scaled to obtain a daily average. A direct use of the coarse spatial resolution CERES measurements would exclude aerosol distributions in partly cloudy CERES scenes. Several approaches that incorporate coincident, high spatial and spectral resolution measurements (e.g., MODIS) have been employed to overcome this limitation (Loeb and Manalo-Smith, 2005; Zhang et al., 2005b).

The Interagency Monitoring of Protected Visual Environment (IMPROVE), which is operated by the National Park Service Air Resources Division, has stations across the US located within national parks (Malm et al., 1994). Although the primary focus of the network is air pollution, the measurements are also relevant to climate forcing research. Measurements include fine and coarse mode (PM2.5 and PM10) aerosol mass concentration; concentrations of elements, sulfate, nitrate, organic carbon, and elemental carbon; and scattering coefficients.

In addition, to these US-operated networks, there are other national and international surface networks that provide measurements of aerosol properties including, but not limited to, the World Meteorological Organization (WMO) Global Atmospheric Watch (GAW) network (http://www.wmo.int/pages/prog/arep/gaw/

Box 2.5: Active Remote Sensing of Aerosols

Following the success of a demonstration of lidar system aboard the U.S. Space Shuttle mission in 1994, i.e., Lidar In-space Technology Experiment (LITE) (Winker et al., 1996), the Geoscience Laser Altimeter System (GLAS) was launched in early 2003 to become the first polar orbiting satellite lidar. It provides global aerosol and cloud profiling for a one-month period out of every three-to-six months. It has been demonstrated that GLAS is capable of detecting and discriminating multiple layer clouds, atmospheric boundary layer aerosols, and elevated aerosol layers (e.g., Spinhirne et al., 2005). The Cloud-Aerosol Lidar and Infrared Pathfinder Satellite Observations (CALIPSO), launched on April 28, 2006, is carrying a lidar instrument (Cloud and Aerosol Lidar with Orthogonal Polarization - CALIOP) that has been collecting profiles of the attenuated backscatter at visible and near-infrared wavelengths along with polarized backscatter in the visible channel (Winker et al., 2003). CALIOP measurements have been used to derive the above-cloud fraction of aerosol extinction optical depth (Chand et al., 2008), one of the important factors determining aerosol direct radiative forcing in cloudy conditions. Figure 2.4 shows an event of trans-Atlantic transport of Saharan dust captured by CALIPSO. Flying in formation with the Aqua, AURA, POLDER, and CloudSat satellites, the vertically resolved information is expected to greatly improve passive aerosol and cloud retrievals as well as allow the retrieval of vertical distributions of aerosol extinction, fine- and coarse-mode separately (Kaufman et al., 2003; Leon et al., 2003; Huneeus and Boucher, 2007).

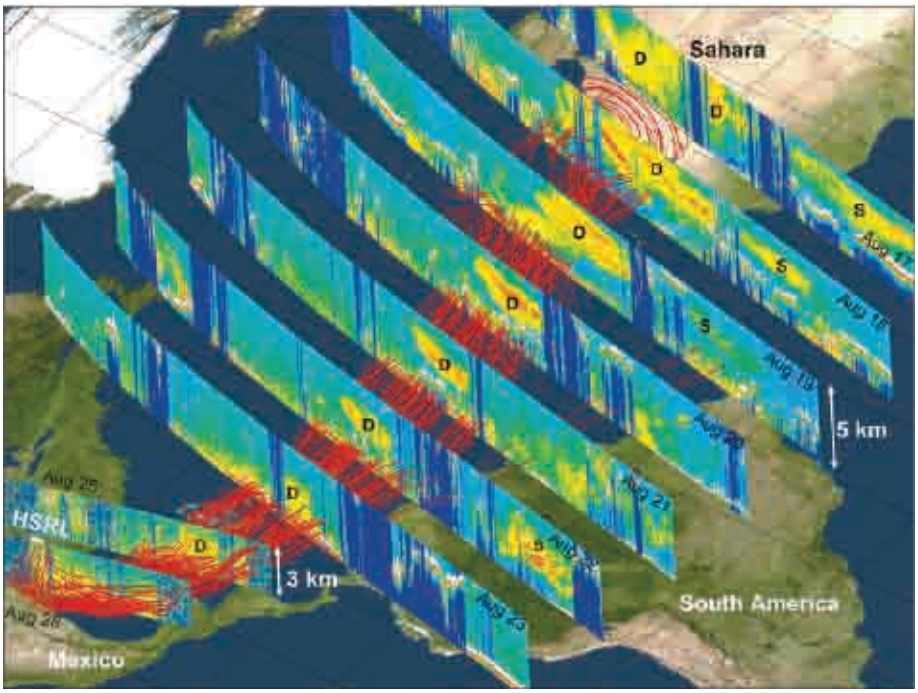

Figure 2.4. A dust event that originated in the Sahara desert on 17 August 2007 and was transported to the Gulf of Mexico. Red lines represent back trajectories indicating the transport track of the dust event. Vertical images are 532 nm attenuated backscatter coefficients measured by CALIOP when passing over the dust transport track. The letter "D" designates the dust layer, and "S" represents smoke layers from biomass burning in Africa (17–19 August) and South America (22 August). The track of the high-spectral-resolution-lidar (HSRL) measurement is indicated by the white line superimposed on the 28 August CALIPSO image. The HSRL track is coincident with the track of the 28 August CALIPSO measurement off the coast of Texas between 28.75°N and 29.08°N (taken from Liu et al., 2008).

monitoring.html), the European Monitoring and Evaluation Programme (EMEP) (http://www.emep.int/), the Canadian Air and Precipitation Monitoring Network (CAPMoN) (http://www.msc-smc.ec.gc.ca/capmon/index_e.cfm), and the Acid Deposition Monitoring Network in East Asia (EANET) (http://www.eanet.cc/eanet.html).

2.2.4. In situ Aerosol Profiling Programs

In addition to long-term ground based measurements, regular long-term aircraft *in situ* measurements recently have been implemented at several locations. These programs provide a statistically significant data set of the vertical distribution of aerosol properties to determine

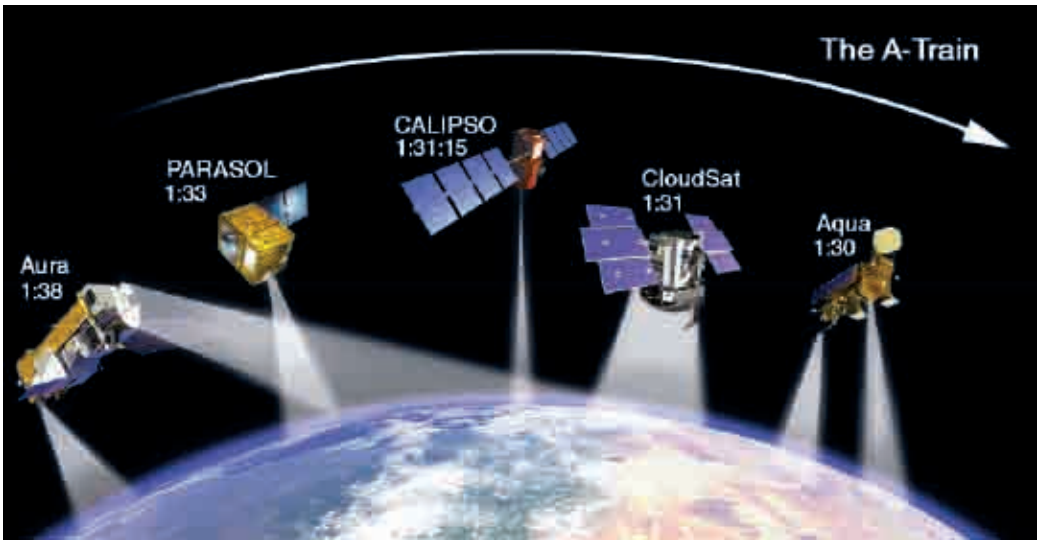

Figure 2.5. A constellation of five spacecraft that overfly the Equator at about 1:30 PM, the so-called A-Train, carries sensors having complementary capabilities, offering unprecedented opportunities to study aerosols from space in multiple dimensions.

spatial and temporal variability through the vertical column and the influence of regional sources on that variability. In addition, the measurements provide data for satellite and model validation. As part of its long-term ground measurements, NOAA has conducted regular flights over Bondville, Illinois since 2006. Measurements include light scattering and absorption coefficients, the relative humidity dependence of light scattering, aerosol number concentration and size distribution, and chemical composition. The same measurements with the exception of number concentration, size distribution, and chemical composition were made by NOAA during regular overflights of DOE ARM's Southern Great Plains (SGP) site from 2000 to 2007 (Andrews et al., 2004) (http://www.esrl.noaa.gov/gmd/aero/net/index.html).

In summary of sections 2.2.2, 2.2.3, and 2.2.4, *in situ* measurements of aerosol properties have greatly expanded over the past two decades as evidenced by the number of focused field campaigns in or downwind of aerosol source regions all over the globe, the continuation of existing and implementation of new sampling networks worldwide, and the implementation of regular aerosol profiling measurements from fixed locations. In addition, *in situ* measurement capabilities have undergone major advancements during this same time period. These advancements include the ability to measure aerosol chemical composition as a function of size at a time resolution of seconds to minutes (e.g., Jayne et al., 2000), the development of instruments able to measure aerosol absorption and extinction coefficients at high sensitivity and time resolution and as a function of relative humidity (e.g., Baynard et al., 2007; Lack et al., 2006), and the deployment of these instruments across the globe on ships, at ground-based sites, and on aircraft. However, further advances are needed to make this newly developed instrumentation more affordable and turn-key so that it can be deployed more widely to characterize aerosol properties at a variety of sites world-wide.

In situ measurements of aerosol properties have greatly expanded over the past two decades as evidenced by the number of focused field campaigns, the world-wide sampling networks, and the regular aerosol profiling measurements from fixed locations.

2.2.5. Ground-based Remote Sensing Measurement Networks

The Aerosol Robotic Network (AERONET) program is a federated ground-based remote sensing network of well-calibrated sun photometers and radiometers (http://aeronet.gsfc.nasa.gov).

AERONET includes about 200 sites around the world, covering all major tropospheric aerosol regimes (Holben et al., 1998; 2001), as illustrated in Figure 2.6. Spectral measurements of sun and sky radiance are calibrated and screened for cloud-free conditions (Smirnov et al., 2000). AERONET stations provide direct, calibrated measurements of spectral AOD (normally at wavelengths of 440, 670, 870, and 1020 nm) with an accuracy of ±0.015 (Eck et al., 1999). In addition, inversion-based retrievals of a variety of effective, column-mean properties have been developed, including aerosol single-scattering albedo, size distributions, fine-mode frac-

Table 2.2. List of major intensive field experiments that are relevant to aerosol research in a variety of aerosol regimes around the globe conducted in the past two decades (updated from Yu et al., 2006).

Aerosol Regimes	Intensive Field Experiments			Major References
	Name	Location	Time Period	
Anthropogenic aerosol and boreal forest from North America and West Europe	TARFOX	North Atlantic	July 1996	Russell et al., 1999
	NEAQS	North Atlantic	July-August 2002	Quinn and Bates, 2003
	SCAR-A	North America	1993	Remer et al., 1997
	CLAMS	East Coast of U.S.	July-August 2001	Smith et al., 2005
	INTEX-NA, ICARTT	North America	Summer 2004	Fehsenfeld et al., 2006
	DOE AIOP	northern Oklahoma	May 2003	Ferrare et al., 2006
	MILAGRO	Mexico city, Mexico	March 2006	Molina et al., 2008
	TexAQS/ GoMACCS	Texas and Gulf of Mexico	August-September 2006	Jiang et al., 2008; Lu et al., 2008
	ARCTAS	North-central Alaska to Greenland (Arctic haze)	March-April 2008	http://www.espo.nasa.gov/arctas/
	ARCTAS	Northern Canada (smoke)	June-July 2008	
	ACE-2	North Atlantic	June-July 1997	Raes et al., 2000
	MINOS	Mediterranean region	July-August 2001	Lelieveld et al., 2002
	LACE98	Lindberg, Germany	July-August 1998	Ansmann et al., 2002
	Aerosols99	Atlantic	January-February 1999	Bates et al., 2001
Brown Haze in South Asia	INDOEX	Indian subcontinent and Indian Ocean	January-April 1998 and 1999	Ramanathan et al., 2001b
	ABC	South and East Asia	ongoing	Ramanathan and Crutzen, 2003
Anthropogenic aerosol and desert dust mixture from East Asia	EAST-AIRE	China	March-April 2005	Li et al., 2007
	INTEX-B	northeastern Pacific	April 2006	Singh et al., 2008
	ACE-Asia	East Asia and Northwest Pacific	April 2001	Huebert et al., 2003; Seinfeld et al., 2004
	TRACE-P		March-April 2001	Jacob et al., 2003
	PEM-West A & B	Western Pacific off East Asia	September-October 1991 February-March 1994	Hoell et al., 1996; 1997
Biomass burning smoke in the tropics	BASE-A	Brazil	1989	Kaufman et al., 1992
	SCAR-B	Brazil	August-September 1995	Kaufman et al., 1998
	LBA-SMOCC	Amazon basin	September-November 2002	Andreae et al., 2004
	SAFARI2000	South Africa and South Atlantic	August -September 2000	King et al., 2003
	SAFARI92		September-October 1992	Lindesay et al., 1996
	TRACE-A	South Atlantic	September-October 1992	Fishman et al., 1996
	DABEX	West Africa	January-February 2006	Haywood et al., 2008
Mineral dusts from North Africa and Arabian Peninsula	SAMUM	Southern Morocco	May-June 2006	Heintzenberg et al., 2009
	SHADE	West coast of North Africa	September 2000	Tanré et al., 2003
	PRIDE	Puerto Rico	June-July 2000	Reid et al., 2003
	UAE[2]	Arabian Peninsula	August-September 2004	Reid et al., 2008
Remote Oceanic Aerosol	ACE-1	Southern Oceans	December 1995	Bates et al., 1998; Quinn and Coffman, 1998

Table 2.3. Summary of major US surface *in situ* and remote sensing networks for the tropospheric aerosol characterization and radiative forcing research. All the reported quantities are column-integrated or column-effective, except as indicated.

Surface Network		Measured/derived parameters				Spatial coverage	Temporal coverage
		Loading	Size, shape	Absorption	Chemistry		
In Situ	NOAA ESRL aerosol monitoring (http://www.esrl.noaa.gov/gmd/aero/)	near-surface extinction coefficient, optical depth, CN/CCN number concentrations	Angstrom exponent, hemispheric backscatter fraction, asymmetry factor, hygroscopic growth	single-scattering albedo, absorption coefficient	chemical composition in selected sites and periods	5 baseline stations, several regional stations, aircraft and mobile platforms	1976 onward
	NPS/EPA IMPROVE (http://vista.cira.colostate.edu/improve/)	near-surface mass concentrations and derived extinction coefficients by species	fine and coarse separately	single-scattering albedo, absorption coefficient	ions, ammonium sulfate, ammonium nitrate, organics, elemental carbon, fine soil	156 national parks and wilderness areas in the U.S.	1988 onward
Remote Sensing	NASA AERONET (http://aeronet.gsfc.nasa.gov)	optical depth	fine-mode fraction, Angstrom exponents, asymmetry factor, phase function, non-spherical fraction	single-scattering albedo, absorption optical depth, refractive indices	N/A	~200 sites over global land and islands	1993 onward
	DOE ARM (http://www.arm.gov)					6 sites and 1 mobile facility in N. America, Europe, and Asia	1989 onward
	NOAA SURFRAD (http://www.srrb.noaa.gov/surfrad/)		N/A	N/A	N/A	7 sites in the U.S.	1995 onward
	AERONET- MAN (http://aeronet.gsfc.nasa.gov/maritime_aerosol_network.html)					global ocean	2004-present (periodically)
	NASA MPLNET (http://mplnet.gsfc.nasa.gov/)	vertical profiles of backscatter/extinction coefficient	N/A	N/A	N/A	~30 sites in major continents, usually collocated with AERONET and ARM sites	2000 onward

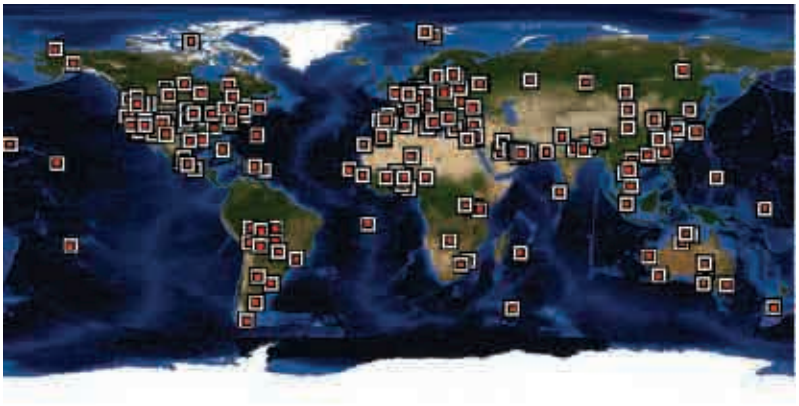

Figure 2.6. Geographical coverage of active AERONET sites in 2006.

AERONET includes about 200 sites around the world, covering all major tropospheric aerosol regimes. AERONET stations provide direct, calibrated measurements of spectral AOD with an accuracy of ±0.015.

tion, degree of non-sphericity, phase function, and asymmetry factor (Dubovik et al., 2000; Dubovik and King, 2000; Dubovik et al., 2002; O'Neill, et al., 2004). The SSA can be retrieved with an accuracy of ±0.03, but only for AOD >0.4 (Dubovik et al., 2002), which precludes much of the planet. These retrieved parameters have been validated or are undergoing validation by comparison to *in situ* measurements (e.g., Haywood et al., 2003; Magi et al., 2005; Leahy et al., 2007).

Recent developments associated with AERONET algorithms and data products include:

- simultaneous retrieval of aerosol and surface properties using combined AERONET and satellite measurements (Sinyuk et al., 2007) with surface reflectance taken into account (which significantly improves AERONET SSA retrieval accuracy) (Eck et al., 2008);
- the addition of ocean color and high frequency solar flux measurements; and
- the establishment of the Maritime Aerosol Network (MAN) component to monitor aerosols over the World oceans from ships-of-opportunity (Smirnov et al., 2006).

Because of consistent calibration, cloud-screening, and retrieval methods, uniformly acquired and processed data are available from all stations, some of which have operated for over 10 years. These data constitute a high-quality, ground-based aerosol climatology and, as such, have been widely used for aerosol process studies as well as for evaluation and validation of model simulation and satellite remote sensing applications (e.g., Chin et al., 2002; Yu et al., 2003, 2006; Remer et al., 2005; Kahn et al., 2005a). In addition, AERONET retrievals of aerosol size distribution and refractive indices have been used in algorithm development for satellite sensors (Remer et al., 2005; Levy et al., 2007a). A set of aerosol optical properties provided by AERONET has been used to calculate the aerosol direct radiative forcing (Procopio et al., 2004; Zhou et al., 2005), which can be used to evaluate both satellite remote sensing measurements and model simulations.

AERONET measurements are complemented by other ground-based aerosol networks having less geographical or temporal coverage, such as the Atmospheric Radiation Measurement (ARM) network (Ackerman and Stokes, 2003), NOAA's national surface radiation budget network (SURFRAD) (Augustine et al., 2008) and other networks with multifilter rotating shadowband radiometer (MFRSR) (Harrison et al., 1994; Michalsky et al., 2001), and several lidar networks including

- NASA Micro Pulse Lidar Network (MPLNET) (Welton et al., 2001; 2002);
- Regional East Atmospheric Lidar Mesonet (REALM) in North America (Hoff et al., 2002; 2004);
- European Aerosol Research Lidar Network (EARLINET) (Matthias et al., 2004); and
- Asian Dust Network (AD-Net) (e.g., Murayama et al., 2001).

Obtaining accurate aerosol extinction profile observations is pivotal to improving aerosol radiative forcing and atmospheric response calculations. The values derived from these lidar networks with state-of-the-art techniques (Schmid et al., 2006) are helping to fill this need.

2.2.6. Synergy of Measurements and Model Simulations

Individual approaches discussed above have their own strengths and limitations, and are usually complementary. None of these approaches alone is adequate to characterize large spatial and temporal variations of aerosol physical and chemical properties and to address complex aerosol-climate interactions. The best strategy for characterizing aerosols and estimating their radiative forcing is to integrate measurements from different satellite sensors with complementary capabilities from *in situ* and surface-based measurements. Similarly, while models are essential tools for estimating regional and global distributions and radiative forcing of aerosols at present as well as in the past and the future, observations are required to provide

constraints and validation of the models. In the following, several synergistic approaches to studying aerosols and their radiative forcing are discussed.

Closure experiments: During intensive field studies, multiple platforms and instruments are deployed to sample regional aerosol properties through a well-coordinated experimental design. Often, several independent methods are used to measure or derive a single aerosol property or radiative forcing. This combination of methods can be used to identify inconsistencies in the methods and to quantify uncertainties in measured, derived, and calculated aerosol properties and radiative forcings. This approach, often referred to as a closure experiment, has been widely employed on both individual measurement platforms (local closure) and in studies involving vertical measurements through the atmospheric column by one or more platforms (column closure) (Quinn et al., 1996; Russell et al., 1997).

Past closure studies have revealed that the best agreement between methods occurs for submicrometer, spherical particles such that different measures of aerosol optical properties and optical depth agree within 10 to 15% and often better (e.g., Clarke et al., 1996; Collins et al., 2000; Schmid et al., 2000; Quinn et al., 2004). Larger particle sizes (e.g., sea salt and dust) present inlet collection efficiency issues and non-spherical particles (e.g., dust) lead to differences in instrumental responses. In these cases, differences between methods for determining aerosol optical depth can be as great as 35% (e.g., Wang et al., 2003; Doherty et al., 2005). Closure studies on aerosol clear-sky DRF reveal uncertainties of about 25% for sulfate/carbonaceous aerosol and 60% for dust-containing aerosol (Bates et al., 2006). Future closure studies could integrate surface- and satellite-based radiometric measurements of AOD with *in situ* optical, microphysical, and aircraft radiometric measurements for a wide range of situations. There is also a need to maintain consistency in comparing results and expressing uncertainties (Bates et al., 2006).

Constraining models with *in situ* measurements: *In situ* measurements of aerosol chemical, microphysical, and optical properties with known accuracy, based in part on closure studies, can be used to constrain regional CTM simulations of aerosol direct forcing, as described by Bates et al. (2006). A key step in the approach is assigning empirically derived optical properties to the individual chemical components generated by the CTM for use in a Radiative Transfer Model (RTM). Specifically, regional data from focused, short-duration field programs can be segregated according to aerosol type (sea salt, dust, or sulfate/carbonaceous) based on measured chemical composition and particle size. Corresponding measured optical properties can be carried along in the sorting process so that they, too, are segregated by aerosol type. The empirically derived aerosol properties for individual aerosol types, including mass scattering efficiency, single-scattering albedo, and asymmetry factor, and their dependences on relative humidity, can be used in place of assumed values in CTMs.

Short-term, focused measurements of aerosol properties (e.g., aerosol concentration and AOD) also can be used to evaluate CTM parameterizations on a regional basis, to suggest improvements to such uncertain model parameters, such as emission factors and scavenging coefficients (e.g., Koch et al., 2007). Improvements in these parameterizations using observations yield increasing confidence in simulations covering regions and periods where and when measurements are not available. To evaluate the aerosol properties generated by CTMs on broader scales in space and time, satellite observations and long-term *in situ* measurements are required.

Improving model simulations with satellite measurements: Global measurements of aerosols from satellites (mainly AOD) with well-defined accuracies offer an opportunity to evaluate model simulations at large spatial and temporal scales. The satellite measurements can also be used to constrain aerosol model simulations and hence the assessment of aerosol DRF through data assimilation or objective analysis process (e.g., Collins et al., 2001; Yu et al., 2003; 2004, 2006; Liu et al., 2005; Zhang et al., 2008). Both satellite retrievals and model simulations have uncertainties. The goal of data integration is to minimize the discrepancies between them, and to form an optimal estimate of aerosol distributions by combining them, typically with weights inversely proportional to the square of the errors of individual descriptions. Such integration can fill gaps in satellite retrievals and

The best strategy for characterizing aerosols and estimating their radiative forcing is to integrate measurements from different satellite sensors with in situ and surface based measurements. Observations are required to provide constraints and validation of the models.

generate global distributions of aerosols that are consistent with ground-based measurements (Collins et al., 2001; Yu et al., 2003, 2006; Liu et al., 2005). Recent efforts have also focused on retrieving global sources of aerosol from satellite observations using inverse modeling, which may be valuable for reducing large aerosol simulation uncertainties (Dubovik et al., 2007). Model refinements guided by model evaluation and integration practices with satellite retrievals can then be used to improve aerosol simulations of the pre- and post-satellite eras.

Current measurement-based understanding of aerosol characterization and radiative forcing is assessed in Section 2.3 through intercomparisons of a variety of measurement-based estimates and model simulations published in literature. This is followed by a detailed discussion of major outstanding issues in section 2.4.

2.3. Assessments of Aerosol Characterization and Climate Forcing

This section focuses on the assessment of measurement-based aerosol characterization and its use in improving estimates of the direct radiative forcing on regional and global scales. *In situ* measurements provide highly accurate aerosol chemical, microphysical, and optical properties on a regional basis and for the particular time period of a given field campaign. Remote sensing from satellites and ground-based networks provide spatial and temporal coverage that intensive field campaigns lack. Both *in situ* measurements and remote sensing have been used to determine key parameters for estimating aerosol direct radiative forcing including aerosol single scattering albedo, asymmetry factor, optical depth Remote sensing has also been providing simultaneous measurements of aerosol optical depth and radiative fluxes that can be combined to derive aerosol direct radiative forcing at the TOA with relaxed requirement for characterizing aerosol properties. Progress in using both satellite and surface-based measurements to study aerosol-cloud interactions and aerosol indirect forcing is also discussed.

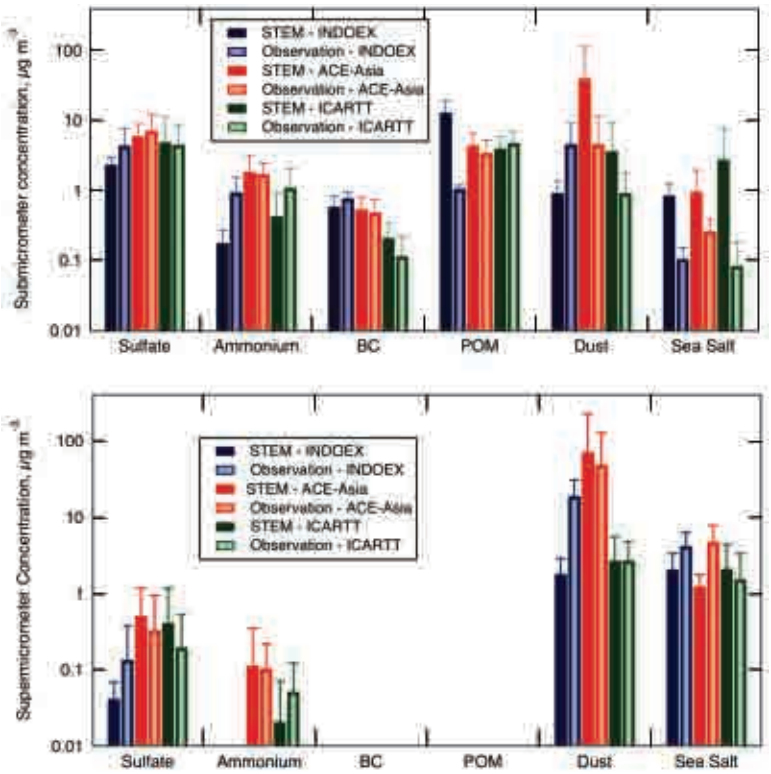

Figure 2.7. Comparison of the mean concentration (μg m-3) and standard deviation of the modeled (STEM) aerosol chemical components with shipboard measurements during INDOEX, ACE-Asia, and ICARTT. After Bates et al. (2006).

2.3.1. The Use of Measured Aerosol Properties to Improve Models

The wide variety of aerosol data sets from intensive field campaigns provides a rigorous "testbed" for model simulations of aerosol properties and distributions and estimates of DRF. As described in Section 2.2.6, *in situ* measurements can be used to constrain regional CTM simulations of aerosol properties, DRF, anthropogenic component of DRF, and to evaluate CTM parameterizations. In addition, *in situ* measurements can be used to develop simplifying parameterizations for use by CTMs.

Several factors contribute to the uncertainty of CTM calculations of size-distributed aerosol composition including emissions, aerosol removal by wet deposition, processes involved in the formation of secondary aerosols and the chemical and microphysical evolution of aerosols, vertical transport, and meteorological fields including the timing and amount of precipitation, formation of clouds, and relative humidity. *In situ* measurements made during focused field campaigns provide a point of comparison for the CTM-generated aerosol distributions at the surface and at discrete points above the surface. Such comparisons are essential for identifying areas where the models need improvement.

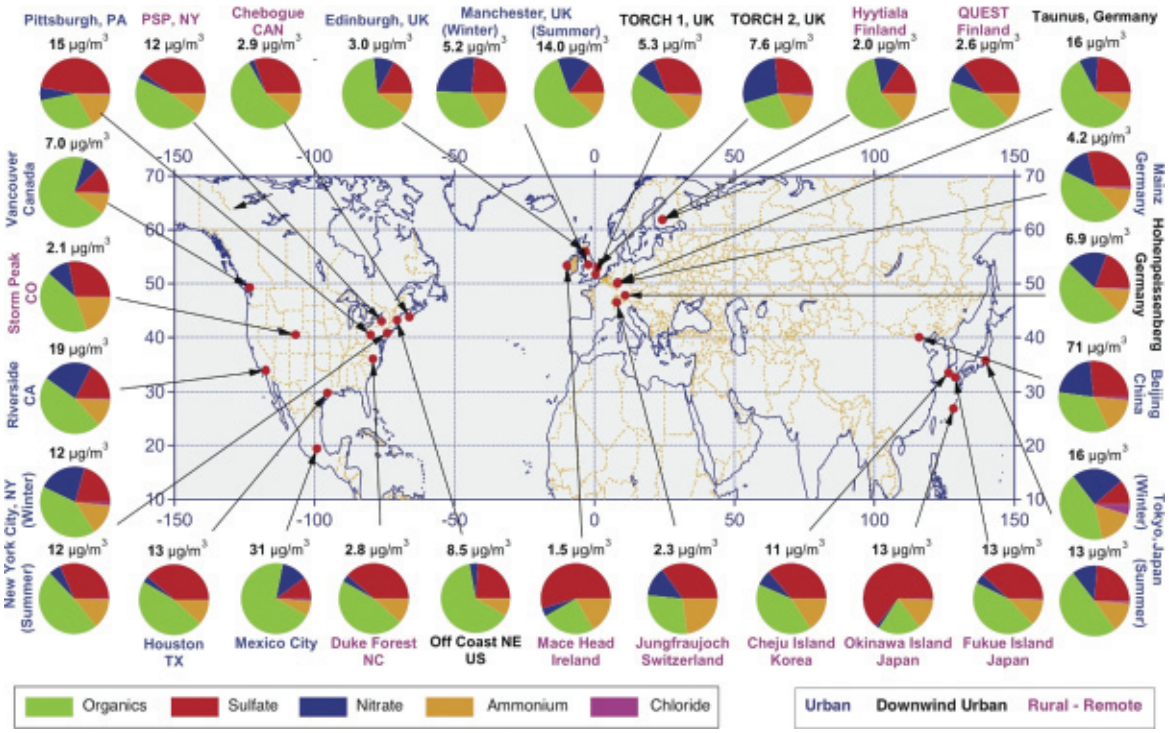

Figure 2.8. Location of aerosol chemical composition measurements with aerosol mass spectrometers. Colors for the labels indicate the type of sampling location: urban areas (blue), <100 miles downwind of major cites (black), and rural/remote areas >100 miles downwind (pink). Pie charts show the average mass concentration and chemical composition: organics (green), sulfate (red), nitrate (blue), ammonium (orange), and chloride (purple), of non-refractory PM1. Adapted from Zhang et al. (2007).

Figure 2.7 shows a comparison of submicrometer and supermicrometer aerosol chemical components measured during INDOEX, ACE-Asia, and ICARTT onboard a ship and the same values calculated with the STEM Model (e.g., Carmichael et al., 2002, 2003; Tang et al., 2003, 2004; Bates et al., 2004; Streets et al., 2006b). To permit direct comparison of the measured and modeled values, the model was driven by analyzed meteorological data and sampled at the times and locations of the shipboard measurements every 30 min along the cruise track. The best agreement was found for submicrometer sulfate and BC. The agreement was best for sulfate; this is attributed to greater accuracy in emissions, chemical conversion, and removal for this component. Underestimation of dust and sea salt is most likely due to errors in model-calculated emissions. Large discrepancies between the modeled and measured values occurred for submicrometer particulate organic matter (POM) (INDOEX), and for particles in the supermicrometer size range such as dust (ACE-Asia), and sea salt (all regions). The model underestimated the total mass of the supermicrometer aerosol by about a factor of 3.

POM makes up a large and variable fraction of aerosol mass throughout the anthropogenically influenced northern hemisphere, and yet models have severe problems in properly representing this type of aerosol. Much of this discrepancy follows from the models inability to represent the formation of secondary organic aerosols (SOA) from the precursor volatile organic compounds (VOC). Figure 2.8 shows a summary of the results from aerosol mass spectrometer measurements at 30 sites over North America, Europe, and Asia. Based on aircraft measurements of urban-influenced air over New England, de Gouw et al. (2005) found that POM was highly correlated with secondary anthropogenic gas phase species suggesting that the POM was derived from secondary anthropogenic sources and that the formation took one day or more.

Particulate organic matter makes up a large and variable fraction of aerosol mass throughout the northern hemisphere, and yet models have severe problems in properly representing this type of aerosol.

Figure 2.9 shows scatterplots of submicrometer POM versus acetylene (a gas phase primary emitted VOC species) and isopropyl nitrate (a secondary gas phase organic species formed by atmospheric reactions). The increase in submicrometer POM with increasing photochemical age could not be explained by the removal of

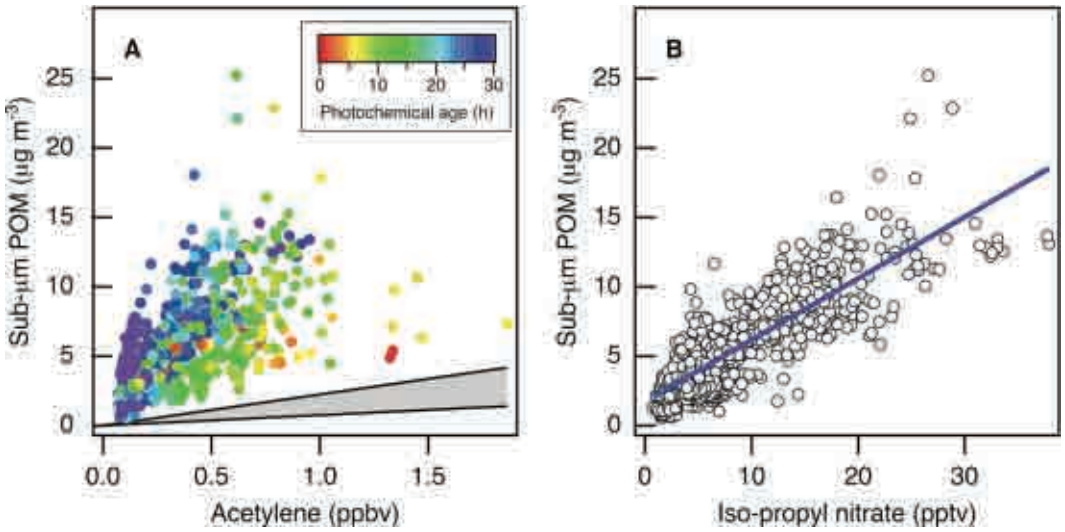

Figure 2.9. Scatterplots of the submicrometer POM measured during NEAQS versus a) acetylene and b) iso-propyl nitrate. The colors of the data points in a) denote the photochemical age as determined by the ratios of compounds of known OH reactivity. The gray area in a) shows the range of ratios between submicrometer POM and acetylene observed by Kirchstetter et al. (1999) in tunnel studies. Adapted from de Guow et al. (2005).

VOC alone, which are its traditionally recognized precursors. This result suggests that other species must have contributed and/or that the mechanism for POM formation is more efficient than assumed by models. Similar results were obtained from the 2006 MILAGRO field campaign conducted in Mexico City (Kleinman et al., 2008), and comparisons of GCM results with several long-term monitoring stations also showed that the model underestimated organic aerosol concentrations (Koch et al., 2007). Recent laboratory work suggests that isoprene may be a major SOA source missing from previous atmospheric models (Kroll et al., 2006; Henze and Seinfeld, 2006), but underestimating sources from certain economic sectors may also play a role (Koch et al., 2007). Models also have difficulty in representing the vertical distribution of organic aerosols, underpredicting their occurrence in the free troposphere (FT) (Heald et al., 2005). While organic aerosol presents models with some of their greatest challenges, even the distribution of well-characterized sulfate aerosol is not always estimated correctly in models (Shindell et al., 2008a).

Comparisons of DRF and its anthropogenic component calculated with assumed optical properties and values constrained by *in situ* measurements can help identify areas of uncertainty in model parameterizations. In a study described by Bates et al. (2006), two different CTMs (MOZART and STEM) were used to calculate dry mass concentrations of the dominant aerosol species (sulfate, organic carbon, black carbon, sea salt, and dust). *In situ* measurements were used to calculate the corresponding optical properties for each aerosol type for use in a radiative transfer model. Aerosol DRF and its anthropogenic component estimated using the empirically derived and *a priori* optical properties were then compared. The DRF and its anthropogenic component were calculated as the net downward solar flux difference between the model state with aerosol and of the model state with no aerosol. It was found that the constrained optical properties derived from measurements increased the calculated AOD (34 ± 8%), TOA DRF (32 ± 12%), and anthropogenic component of TOA DRF (37 ± 7%) relative to runs using the *a priori* values. These increases were due to larger values of the constrained mass extinction efficiencies relative to the *a priori* values. In addition, differences in AOD due to using the aerosol loadings from MOZART versus those from STEM were much greater than differences resulting from the *a priori* vs. constrained RTM runs.

In situ observations also can be used to generate simplified parameterizations for CTMs and RTMs thereby lending an empirical foundation to uncertain parameters currently in use by models. CTMs generate concentration fields of individual aerosol chemical components that are then used as input to radiative transfer models (RTMs) for the calculation of DRF. Currently, these calculations are performed with a variety of simplifying assumptions concerning the RH dependence of light scattering by the aerosol. Chemical components often are treated as externally mixed each with a unique RH dependence of light scattering. However, both model and measurement studies reveal that POM, internally mixed with

water-soluble salts, can reduce the hygroscopic response of the aerosol, which decreases its water content and ability to scatter light at elevated relative humidity (e.g., Saxena et al., 1995; Carrico et al., 2005). The complexity of the POM composition and its impact on aerosol optical properties requires the development of simplifying parameterizations that allow for the incorporation of information derived from field measurements into calculations of DRF (Quinn et al., 2005). Measurements made during INDOEX, ACE-Asia, and ICARTT revealed a substantial decrease in $f_{\sigma sp}(RH)$ with increasing mass fraction of POM in the accumulation mode. Based on these data, a parameterization was developed that quantitatively describes the relationship between POM mass fraction and $f_{\sigma sp}(RH)$ for accumulation mode sulfate-POM mixtures (Quinn et al., 2005). This simplified parameterization may be used as input to RTMs to derive values of $f_{\sigma sp}(RH)$ based on CTM estimates of the POM mass fraction. Alternatively, the relationship may be used to assess values of $f_{\sigma sp}(RH)$ currently being used in RTMs.

2.3.2. Intercomparisons of Satellite Measurements and Model Simulation of Aerosol Optical Depth

As aerosol DRF is highly dependent on the amount of aerosol present, it is of first-order importance to improve the spatial characterization of AOD on a global scale. This requires an evaluation of the various remote sensing AOD data sets and comparison with model-based AOD estimates. The latter comparison is particularly important if models are to be used in projections of future climate states that would result from assumed future emissions. Both remote sensing and model simulation have uncertainties and satellite-model integration is needed to obtain an optimum description of aerosol distribution.

Figure 2.10 shows an intercomparison of annual average AOD at 550 nm from two recent satellite aerosol sensors (MODIS and MISR), five model simulations (GOCART, GISS, SPRINTARS, LMDZ-LOA, LMDZ-INCA) and three satellite-model integrations (MO_GO, MI_GO, MO_MI_GO). These model-satellite integrations are conducted by using an optimum interpolation approach (Yu et al., 2003) to constrain GOCART simulated AOD with that from MODIS, MISR, or MODIS over ocean and MISR over land, denoted as MO_GO, MI_GO, and MO_MI_GO, respectively. MODIS values of AOD are from Terra Collection 4 retrievals and MISR AOD is based on early post launch retrievals. MODIS and MISR retrievals give a comparable average AOD on the global scale, with MISR greater than MODIS by 0.01~0.02 depending on the season. However, differences between MODIS and MISR are much larger when land and ocean are examined separately: AOD from MODIS is 0.02-0.07 higher over land but 0.03-0.04 lower over ocean than the AOD from MISR. Several major causes for the systematic MODIS-MISR differences have been identified, including instrument calibration and sampling differences, different assumptions about ocean surface boundary conditions made in the individual retrieval algorithms, missing particle property or mixture options in the look-up tables, and cloud screening (Kahn

As aerosol direct radiative forcing is highly dependent on the amount of aerosol present, it is of first-order importance to improve the spatial characterization of aerosol optical depth on a global scale.

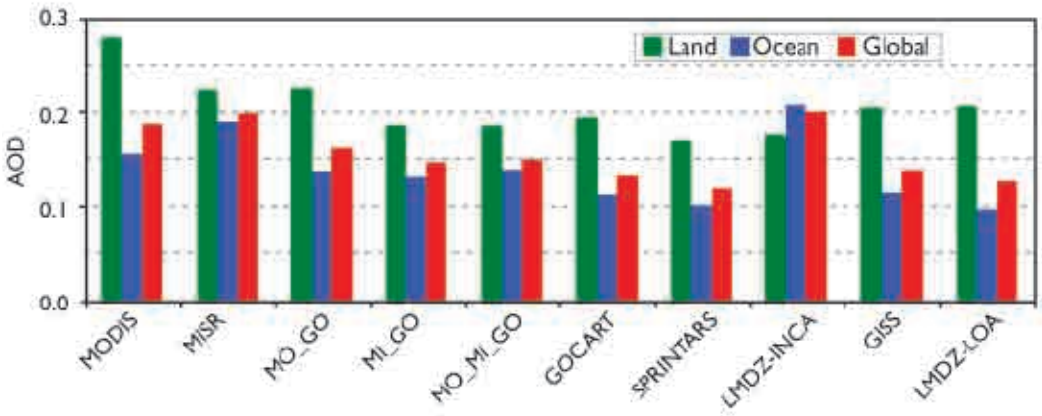

Figure 2.10. Comparison of annual mean aerosol optical depth (AOD) at 550 nm between satellite retrievals (MODIS, MISR), model simulations (GOCART, SPRINTARS, GISS, LMDZ-INCA, LMDZ-LOA), and satellite-model integrations (MO_GO, MI_GO, MO_MI_GO) averaged over land, ocean, and globe (all limited to 60°S-60°N region) (figure generated from Table 6 in Yu et al., 2006).

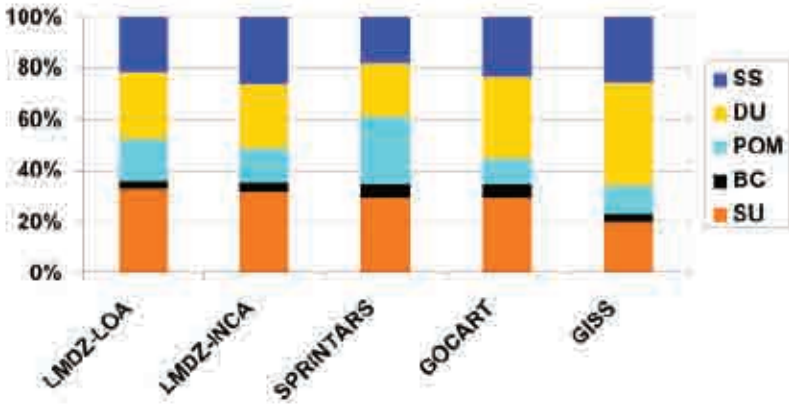

Figure 2.11. Percentage contributions of individual aerosol components (SU – sulfate, BC – black carbon, POM – particulate organic matter, DU – dust, SS – sea salt) to the total aerosol optical depth (at 550 nm) on a global scale simulated by the five models (data taken from Kinne et al., 2006).

et al., 2007b). The MODIS-MISR AOD differences are being reduced by continuous efforts on improving satellite retrieval algorithms and radiance calibration. The new MODIS aerosol retrieval algorithms in Collection 5 have resulted in a reduction of 0.07 for global land mean AOD (Levy et al., 2007b), and improved radiance calibration for MISR removed ~40% of AOD bias over dark water scenes (Kahn et al., 2005b).

The annual and global average AOD from the five models is 0.19±0.02 (mean ± standard deviation) over land and 0.13±0.05 over ocean, respectively. Clearly, the model-based mean AOD is smaller than both MODIS- and MISR-derived values (except the GISS model). A similar conclusion has been drawn from more extensive comparisons involving more models and satellites (Kinne et al., 2006). On regional scales, satellite-model differences are much larger. These differences could be attributed in part to cloud contamination (Kaufman et al., 2005b; Zhang et al., 2005c) and 3D cloud effects in satellite retrievals (Kaufman et al., 2005b; Wen et al., 2006) or to models missing important aerosol sources/sinks or physical processes (Koren et al., 2007b). Integrated satellite-model products are generally in-between the satellite retrievals and the model simulations, and agree better with AERONET measurements (e.g., Yu et al., 2003).

As in comparisons between models and *in situ* measurements (Bates et al., 2006), there appears to be a relationship between uncertainties in the representation of dust in models and the uncertainty in AOD, and its global distribution. For example, the GISS model generates more dust than the other models (Fig. 2.11), resulting in a closer agreement with MODIS and MISR in the global mean (Fig. 2.10). However, the distribution of AOD between land and ocean is quite different from MODIS- and MISR-derived values.

Figure 2.11 shows larger model differences in the simulated percentage contributions of individual components to the total aerosol optical depth on a global scale, and hence in the simulated aerosol single-scattering properties (e.g., single-scattering albedo, and phase function), as documented in Kinne et al. (2006). This, combined with the differences in aerosol loading (as characterized by AOD) determines the model diversity in simulated aerosol direct radiative forcing, as discussed later. However, current satellite remote sensing capability is not sufficient to constrain model simulations of aerosol components.

2.3.3. Satellite Based Estimates of Aerosol Direct Radiative Forcing

Table 2.4 summarizes approaches to estimating the aerosol direct radiative forcing, including a brief description of methods, identifies major sources of uncertainty, and provides references. These estimates fall into three broad categories, namely (A) satellite-based, (B) satellite-model integrated, and (C) model-based. As satellite aerosol measurements are generally limited to cloud-free conditions, the discussion here focuses on assessments of clear-sky aerosol direct radiative forcing, a net (downwelling minus upwelling) solar flux difference between with aerosol (natural + anthropogenic) and in the absence of aerosol.

Global distributions. Figure 2.12 shows global distributions of aerosol optical depth at 550 nm (left panel) and diurnally averaged clear-sky TOA DRF (right panel) for March-April-May (MAM) based on the different approaches. The DRF at the surface follows the same pattern as that at the TOA but is significantly larger in magnitude because of aerosol absorption. It appears that different approaches agree on large-scale patterns of aerosol optical depth and the direct radiative forcing. In this season, the aerosol impacts in the Northern Hemisphere are much larger than those in the Southern Hemisphere. Dust outbreaks and biomass burning elevate the optical depth to more than 0.3 over

Table 2.4. Summary of approaches to estimating the aerosol direct radiative forcing in three categories: (A) satellite retrievals; (B) satellite-model integrations; and (C) model simulations. (adapted from Yu et al., 2006).

Category	Product	Brief Descriptions	Identified Sources of Uncertainty	Major References
A. Satellite retrievals	MODIS	Using MODIS retrievals of a linked set of AOD, ω_0, and phase function consistently in conjunction with a radiative transfer model (RTM) to calculate TOA fluxes that best match the observed radiances.	Radiance calibration, cloud-aerosol discrimination, instantaneous-to-diurnal scaling, RTM parameterizations	Remer and Kaufman, 2006
	MODIS_A	Splitting MODIS AOD over ocean into mineral dust, sea salt, and biomass-burning and pollution; using AERONET measurements to derive the size distribution and single-scattering albedo for individual components.	Satellite AOD and FMF retrievals, overestimate due to summing up the compositional direct forcing, use of a single AERONET site to characterize a large region	Bellouin et al., 2005
	CERES_A	Using CERES fluxes in combination with standard MODIS aerosol.	Calibration of CERES radiances, large CERES footprint, satellite AOD retrieval, radiance-to-flux conversion (ADM), instantaneous-to-diurnal scaling, narrow-to-broadband conversion	Loeb and Manalo-Smith, 2005; Loeb and Kato, 2002
	CERES_B	Using CERES fluxes in combination with NOAA NESDIS aerosol from MODIS radiances.		
	CERES_C	Using CERES fluxes in combination with MODIS (ocean) and MISR (non-desert land) aerosol with new angular models for aerosols.		Zhang et al., 2005a,b; Zhang and Christopher, 2003; Christopher et al., 2006; Patadia et al., 2008
	POLDER	Using POLDER AOD in combination with prescribed aerosol models (similar to MODIS).	Similar to MODIS	Boucher and Tanré, 2000; Bellouin et al., 2003
B. Satellite-model integrations	MODIS_G	Using GOCART simulations to fill AOD gaps in satellite retrievals.	Propagation of uncertainties associated with both satellite retrievals and model simulations (but the model-satellite integration approach does result in improved AOD quality for MO_GO, and MO_MI_GO)	*Aerosol single-scattering albedo and asymmetry factor are taken from GOCART simulations; *Yu et al., 2003, 2004, 2006
	MISR_G			
	MO_GO	Integration of MODIS and GOCART AOD.		
	MO_MI_GO	Integration of GOCART AOD with retrievals from MODIS (Ocean) and MISR (Land).		
	SeaWiFS	Using SeaWiFS AOD and assumed aerosol models.	Similar to MODIS_G and MISR_G, too weak aerosol absorption	Chou et al., 2002
C. Model simulations	GOCART	Offline RT calculations using monthly average aerosols with a time step of 30 min (without the presence of clouds).	Emissions, parameterizations of a variety of sub-grid aerosol processes (e.g., wet and dry deposition, cloud convection, aqueous-phase oxidation), assumptions on aerosol size, absorption, mixture, and humidification of particles, meteorology fields, not fully evaluated surface albedo schemes, RT parameterizations	Chin et al., 2002; Yu et al., 2004
	SPRINTARS	Online RT calculations every 3 hrs (cloud fraction=0).		Takemura et al., 2002, 2005
	GISS	Online model simulations and weighted by clear-sky fraction.		Koch and Hansen, 2005; Koch et al., 2006
	LMDZ-INCA	Online RT calculations every 2 hrs (cloud fraction = 0).		Balkanski et al., 2007; Schulz et al., 2006; Kinne et al., 2006
	LMDZ-LOA	Online RT calculations every 2 hrs (cloud fraction=0).		Reddy et al., 2005a, b

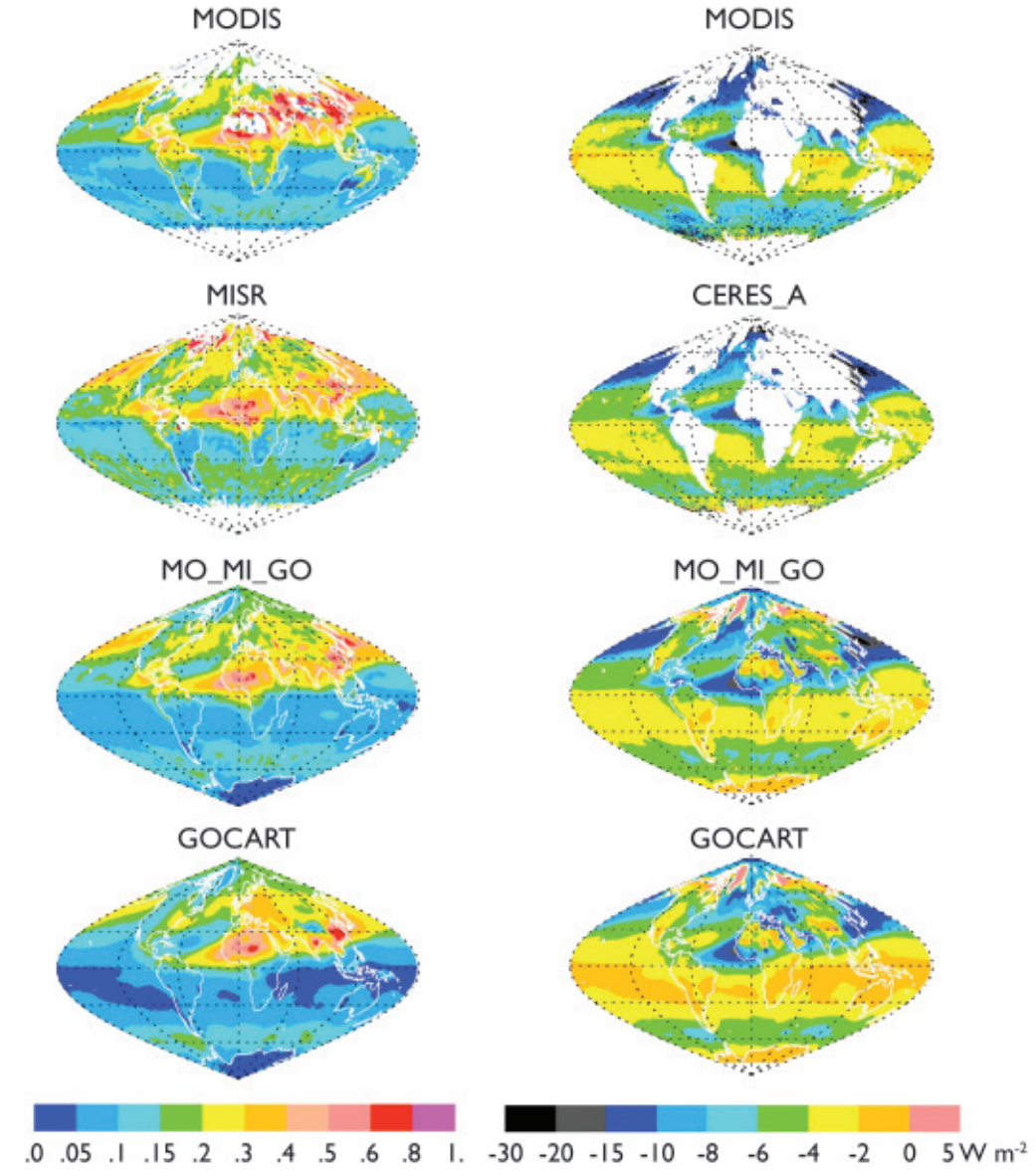

Figure 2.12. Geographical patterns of seasonally (MAM) averaged aerosol optical depth at 550 nm (left panel) and the diurnally averaged clear-sky aerosol direct radiative (solar spectrum) forcing (W m^{-2}) at the TOA (right panel) derived from satellite (Terra) retrievals (MODIS, Remer et al., 2005; Remer and Kaufman, 2006; MISR, Kahn et al., 2005a; and CERES_A, Loeb and Manalo-Smith, 2005), GOCART simulations (Chin et al., 2002; Yu et al., 2004), and GOCART-MODIS-MISR integrations (MO_MI_GO, Yu et al., 2006) (taken from Yu et al., 2006).

large parts of North Africa and the tropical Atlantic. In the tropical Atlantic, TOA cooling as large as -10 W m^{-2} extends westward to Central America. In eastern China, the optical depth is as high as 0.6-0.8, resulting from the combined effects of industrial activities and biomass burning in the south, and dust outbreaks in the north. The Asian impacts also extend to the North Pacific, producing a TOA cooling of more than -10 W m^{-2}. Other areas having large aerosol impacts include Western Europe, midlatitude North Atlantic, and much of South Asia and the Indian Ocean. Over the "roaring forties" in the Southern Hemisphere, high winds generate a large amount of sea salt. Elevated optical depth, along with high solar zenith angle and hence large backscattering to space, results in a band of TOA cooling of more than -4 W m^{-2}. However, there is also some question as to whether thin cirrus (e.g., Zhang et al., 2005c) and unaccounted-for whitecaps contribute to the apparent enhancement in AOD retrieved by satellite. Some differences exist between different approaches. For example, the early

post-launch MISR retrieved optical depths over the southern hemisphere oceans are higher than MODIS retrievals and GOCART simulations. Over the "roaring forties", the MODIS derived TOA solar flux perturbations are larger than the estimates from other approaches.

Global mean. Figure 2.13 summarizes the measurement- and model-based estimates of clear-sky annual-averaged DRF at both the TOA and surface from 60°S to 60°N. Seasonal DRF values for individual estimates are summarized in Table 2.5 and Table 2.6 for ocean and land, respectively. Mean, median and standard error ε ($\varepsilon=\sigma/(n-1)^{1/2}$), where σ is standard deviation and n is the number of methods) are calculated for measurement- and model-based estimates separately. Note that although the standard deviation or standard error reported here is not a fully rigorous measure of a true experimental uncertainty, it is indicative of the uncertainty because independent approaches with independent sources of errors are used (see Table 2.4; in the modeling community, this is called the "diversity", see Chapter 3).

- **Ocean:** For the TOA DRF, a majority of measurement-based and satellite-model integration-based estimates agree with each other within about 10%. On annual average, the measurement-based estimates give the DRF of -5.5±0.2 W m^{-2} (mean±ε) at the TOA and -8.7±0.7 W m^{-2} at the surface. This suggests that the ocean surface cooling is about 60% larger than the cooling at the TOA. Model simulations give wide ranges of DRF estimates at both the TOA and surface. The ensemble of five models gives the annual average DRF (mean ± ε) of -3.2±0.6 W m^{-2} and -4.9±0.8 W m^{-2} at the TOA and surface, respectively. On average, the surface cooling is about 37% larger than the TOA cooling, smaller than the measurement-based estimate of surface and TOA difference of 60%. However, the 'measurement-based' estimate of *surface* DRF is actually a calculated value, using poorly constrained particle properties.
- **Land:** It remains challenging to use satellite measurements alone for characterizing complex aerosol properties over land surfaces with high accuracy. As such, DRF estimates over land have to rely largely on model simulations and satellite-model integrations. On a global and annual average, the satellite-model integrated approaches derive a mean DRF of -4.9 W m^{-2} at the TOA and -11.9 W m^{-2} at the surface respectively. The surface cooling is more than a factor of 2 larger than the TOA cooling because of aerosol absorption. Note that the TOA DRF of -4.9 W m^{-2} agrees quite well with the most recent satellite-based estimate of -5.1±1.1 W m^{-2} over non-desert land based on coincident measurements of MISR AOD and CERES solar flux (Patadia et al., 2008). For comparisons, an ensemble of five model simulations derives a DRF (mean ± ε) over land of -3.0±0.6 W m^{-2} at the TOA and -7.6±0.9 W m^{-2} at the surface, respectively. Seasonal variations of DRF over land, as derived from both measurements and models, are larger than those over ocean.

The above analyses show that, on a global average, the measurement-based estimates of DRF are 55-80% greater than the model-based estimates. The differences are even larger on regional scales. Such measurement-model differences are a combination of differences in aerosol amount (optical depth), single-scattering properties, surface albedo, and radiative transfer schemes (Yu et al., 2006). As discussed earlier, MODIS retrieved optical depths tend to be overestimated by about 10-15% due to the contamination of thin cirrus and clouds in

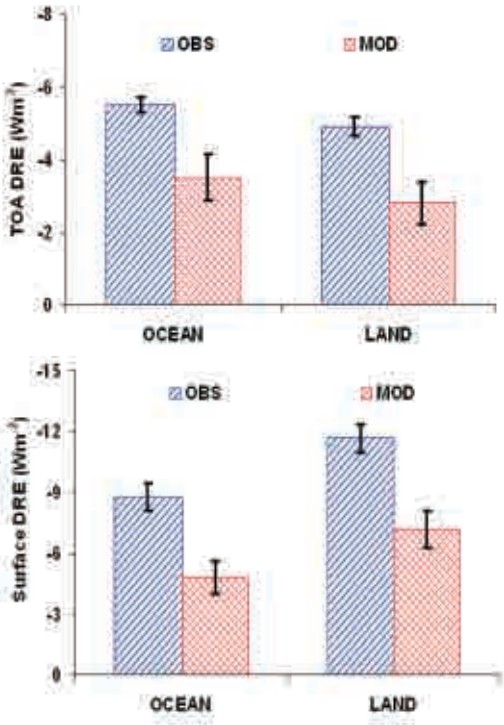

Figure 2.13. Summary of observation- and model-based (denoted as OBS and MOD, respectively) estimates of clear-sky, annual average DRF at the TOA and at the surface. The box and vertical bar represent median and standard error, respectively. (taken from Yu et al., 2006).

Table 2.5. Summary of seasonal and annual average clear-sky DRF (W m^{-2}) at the TOA and the surface (SFC) over global OCEAN derived with different methods and data. Sources of data: MODIS (Remer & Kaufman, 2006), MODIS_A (Bellouin et al., 2005), POLDER (Boucher and Tanré, 2000; Bellouin et al., 2003), CERES_A and CERES_B (Loeb and Manalo-Smith, 2005), CERES_C (Zhang et al., 2005b), MODIS_G, MISR_G, MO_GO, MO_MI_GO (Yu et al., 2004; 2006), SeaWiFS (Chou et al., 2002), GOCART (Chin et al., 2002; Yu et al., 2004), SPRINTARS (Takemura et al., 2002), GISS (Koch and Hansen, 2005; Koch et al., 2006), LMDZ-INCA (Kinne et al., 2006; Schulz et al., 2006), LMDZ-LOA (Reddy et al., 2005a, b). Mean, median, standard deviation (σ), and standard error (ε) are calculated for observations (Obs) and model simulations (Mod) separately. The last row is the ratio of model median to observational median. (taken from Yu et al., 2006)

Products	DJF		MAM		JJA		SON		ANN	
	TOA	SFC	TOA	SFC	TOA	SFC	TOA	SFC	TOA	SFC
MODIS	-5.9		-5.8		-6.0		-5.8		-5.9	
MODIS_A*	-6.0	-8.2	-6.4	-8.9	-6.5	-9.3	-6.4	-8.9	-6.4	-8.9
CERES_A	-5.2		-6.1		-5.4		-5.1		-5.5	
CERES_B	-3.8		-4.3		-3.5		-3.6		-3.8	
CERES_C	-5.3		-5.4		-5.2				-5.3	
MODIS_G	-5.5	-9.1	-5.7	-10.4	-6.0	-10.6	-5.5	-9.8	-5.7	-10.0
MISR_G**	-6.4	-10.3	-6.5	-11.4	-7.0	-11.9	-6.3	-10.9	-6.5	-11.1
MO_GO	-4.9	-7.8	-5.1	-9.3	-5.4	-9.4	-5.0	-8.7	-5.1	-8.8
MO_MI_GO	-4.9	-7.9	-5.1	-9.2	-5.5	-9.5	-5.0	-8.6	-5.1	-8.7
POLDER	-5.7		-5.7		-5.8		-5.6		-5.7 -5.2***	 -7.7***
SeaWiFS	-6.0	-6.6	-5.2	-5.8	-4.9	-5.6	-5.3	-5.7	-5.4	-5.9
Obs. Mean	-5.4	-8.3	-5.6	-9.2	-5.6	-9.4	-5.4	-8.8	-5.5	-8.7
Obs. Median	-5.5	-8.1	-5.7	-9.3	-5.5	-9.5	-5.4	-8.8	-5.5	-8.8
Obs. σ	0.72	1.26	0.64	1.89	0.91	2.10	0.79	1.74	0.70	1.65
Obs. ε	0.23	0.56	0.20	0.85	0.29	0.94	0.26	0.78	0.21	0.67
GOCART	-3.6	-5.7	-4.0	-7.2	-4.7	-8.0	-4.0	-6.8	-4.1	-6.9
SPRINTARS	-1.5	-2.5	-1.5	-2.5	-1.9	-3.3	-1.5	-2.5	-1.6	-2.7
GISS	-3.3	-4.1	-3.5	-4.6	-3.5	-4.9	-3.8	-5.4	-3.5	-4.8
LMDZ -INCA	-4.6	-5.6	-4.7	-5.9	-5.0	-6.3	-4.8	-5.5	-4.7	-5.8
LMDZ -LOA	-2.2	-4.1	-2.2	-3.7	-2.5	-4.4	-2.2	-4.1	-2.3	-4.1
Mod. Mean	-3.0	-4.4	-3.2	-4.8	-3.5	-5.4	-3.3	-4.9	-3.2	-4.9
Mod. Median	-3.3	-4.1	-3.5	-4.6	-3.5	-4.9	-3.8	-5.4	-3.5	-4.8
Mod. σ	1.21	1.32	1.31	1.84	1.35	1.82	1.36	1.63	1.28	1.6
Mod. ε	0.61	0.66	0.66	0.92	0.67	0.91	0.68	0.81	0.64	0.80
Mod./Obs.	0.60	0.51	0.61	0.50	0.64	0.52	0.70	0.61	0.64	0.55

* High bias may result from adding the DRF of individual components to derive the total DRF (Bellouin et al., 2005).
** High bias most likely results from an overall overestimate of 20% in early post-launch MISR optical depth retrievals (Kahn et al., 2005).
*** Bellouin et al. (2003) use AERONET retrieval of aerosol absorption as a constraint to the method in Boucher and Tanré (2000), deriving aerosol direct radiative forcing both at the TOA and the surface.

general (Kaufman et al., 2005b). Such overestimation of optical depth would result in a comparable overestimate of the aerosol direct radiative forcing. Other satellite AOD data may have similar contamination, which however has not yet been quantified. On the other hand, the observations may be measuring enhanced AOD and DRF due to processes not well represented in the models including humidification and enhancement of aerosols in the vicinity of clouds (Koren et al., 2007b).

From the perspective of model simulations, uncertainties associated with parameterizations of various aerosol processes and meteorological fields, as documented under the AEROCOM and Global Modeling Initiative (GMI) frameworks (Kinne et al., 2006; Textor et al., 2006; Liu et al., 2007), contribute to the large measurement-model and model-model discrepancies. Factors determining the AOD should be major reasons for the DRF discrepancy and the constraint of model AOD with well evaluated and bias reduced satellite AOD through a data assimilation approach can reduce the DRF discrepancy significantly. Other factors (such as model parameterization of surface reflectance, and model-satellite differences in single-scattering albedo and asymmetry factor due to satellite sampling bias toward cloud-free conditions) should also contribute, as evidenced by the existence of a large discrepancy in the radiative efficiency (Yu et al., 2006). Significant effort will be needed in the future to conduct comprehensive assessments.

On a global average, the measurement-based estimates of aerosol direct radiative forcing are 55-80% greater than the model-based estimates. The differences are even larger on regional scales.

Table 2.6. Summary of seasonal and annual average clear-sky DRF (W m^{-2}) at the TOA and the surface (SFC) over global LAND derived with different methods and data. Sources of data: MODIS_G, MISR_G, MO_GO, MO_MI_GO (Yu et al., 2004, 2006), GOCART (Chin et al., 2002; Yu et al., 2004), SPRINTARS (Takemura et al., 2002), GISS (Koch and Hansen, 2005; Koch et al., 2006), LMDZ-INCA (Balkanski et al., 2007; Kinne et al., 2006; Schulz et al., 2006), LMDZ-LOA (Reddy et al., 2005a, b). Mean, median, standard deviation (σ), and standard error (ε) are calculated for observations (Obs) and model simulations (Mod) separately. The last row is the ratio of model median to observational median. (taken from Yu et al., 2006)

Products	DJF		MAM		JJA		SON		ANN	
	TOA	SFC	TOA	SFC	TOA	SFC	TOA	SFC	TOA	SFC
MODIS_G	-4.1	-9.1	-5.8	-14.9	-6.6	-17.4	-5.4	-12.8	-5.5	-13.5
MISR_G	-3.9	-8.7	-5.1	-13.0	-5.8	-14.6	-4.6	-10.7	-4.9	-11.8
MO_GO	-3.5	-7.5	-5.1	-12.9	-5.8	-14.9	-4.8	-10.9	-4.8	-11.6
MO_MI_GO	-3.4	-7.4	-4.7	-11.8	-5.3	-13.5	-4.3	-9.7	-4.4	-10.6
Obs. Mean	-3.7	-8.2	-5.2	-13.2	-5.9	-15.1	-4.8	-11.0	-4.9	-11.9
Obs. Median	-3.7	-8.1	-5.1	-13.0	-5.8	-14.8	-4.7	-10.8	-4.9	-11.7
Obs. σ	0.33	0.85	0.46	1.29	0.54	1.65	0.46	1.29	0.45	1.20
Obs. ε	0.17	0.49	0.26	0.74	0.31	0.85	0.27	0.75	0.26	0.70
GOCART	-2.9	-6.1	-4.4	-10.9	-4.8	-12.3	-4.3	-9.3	-4.1	-9.7
SPRINTARS	-1.4	-4.0	-1.5	-4.6	-2.0	-6.7	-1.7	-5.2	-1.7	-5.1
GISS	-1.6	-3.9	-3.2	-7.9	-3.6	-9.3	-2.5	-6.6	-2.8	-7.2
LMDZ-INCA	-3.0	-5.8	-4.0	-9.2	-6.0	-13.5	-4.3	-8.2	-4.3	-9.2
LMDZ-LOA	-1.3	-5.4	-1.8	-6.4	-2.7	-8.9	-2.1	-6.7	-2.0	-6.9
Mod. Mean	-2.0	-5.0	-3.0	-7.8	-3.8	-10.1	-3.0	-7.2	-3.0	-7.6
Mod. Median	-1.6	-5.4	-3.2	-7.9	-3.6	-9.3	-2.5	-6.7	-2.8	-7.2
Mod. σ	0.84	1.03	1.29	2.44	1.61	2.74	1.24	1.58	1.19	1.86
Mod. ε	0.42	0.51	0.65	1.22	0.80	1.37	0.62	0.79	0.59	0.93
Mod./Obs.	0.43	0.67	0.63	0.61	0.62	0.63	0.53	0.62	0.58	0.62

2.3.4. Satellite Based Estimates of Anthropogenic Component of Aerosol Direct Radiative Forcing

Satellite instruments do not measure the aerosol chemical composition needed to discriminate anthropogenic from natural aerosol components. Because anthropogenic aerosols are predominantly sub-micron, the fine-mode fraction derived from POLDER, MODIS, or MISR might be used as a tool for deriving anthropogenic aerosol optical depth. This could provide a feasible way to conduct measurement-based estimates of anthropogenic component of aerosol direct radiative forcing (Kaufman et al., 2002a). Such method derives anthropogenic AOD from satellite measurements by empirically correcting contributions of natural sources (dust and maritime aerosol) to the sub-micron AOD (Kaufman et al., 2005a). The MODIS-based estimate of anthropogenic AOD is about 0.033 over oceans, consistent with model assessments of 0.030~0.036 even though the total AOD from MODIS is 25-40% higher than the models (Kaufman et al., 2005a). This accounts for 21±7% of the MODIS-observed total aerosol optical depth, compared with about 33% of anthropogenic contributions estimated by the models. The anthropogenic fraction of AOD should be much larger over land (i.e., 47±9% from a composite of several models) (Bellouin et al., 2005), comparable to the 40% estimated by Yu et al. (2006). Similarly, the non-spherical fraction from MISR or POLDER can be used to separate dust from spherical aerosol (Kahn et al., 2001; Kalashnikova and Kahn, 2006), providing another constraint for distinguishing anthropogenic from natural aerosols.

Uncertainties in estimates of the anthropogenic component of aerosol direct radiative forcing are greater than for the total aerosol, particularly over land.

There have been several estimates of anthropogenic component of DRF in recent years. Table 2.7 lists such estimates of anthropogenic component of TOA DRF that are from model simulations (Schulz et al., 2006) and constrained to some degree by satellite observations (Kaufman et al., 2005a; Bellouin et al., 2005, 2008; Chung et al., 2005; Christopher et al., 2006; Matsui and Pielke, 2006; Yu et al., 2006; Quaas et al., 2008; Zhao et al., 2008b). The satellite-based clear-sky DRF by anthropogenic aerosols is estimated to be -1.1 ± 0.37 W m^{-2} over ocean, about a factor of 2 stronger than model simulated -0.6 W m^{-2}. Similar DRF estimates are rare over land, but a few studies do suggest that the anthropogenic DRF over land is much more negative than that over ocean (Yu et al., 2006; Bellouin et al., 2005, 2008). On global average, the measurement-based estimate of anthropogenic DRF ranges from -0.9 to -1.9 W m^{-2}, again stronger than the model-based estimate of -0.8 W m^{-2}. Similar to DRF estimates for total aerosols, satellite-based estimates of anthropogenic component of DRF are rare over land.

On global average, anthropogenic aerosols are generally more absorptive than natural aerosols. As such the anthropogenic component of DRF is much more negative at the surface than at TOA. Several observation-constrained studies estimate that the global average, clear-sky, anthropogenic component of DRF at the surface ranges from -4.2 to -5.1 W m^{-2} (Yu et al., 2004; Bellouin et al., 2005; Chung et al., 2005; Matsui and Pielke, 2006), which is about a factor of 2 larger in magnitude than the model estimates (e.g., Reddy et al., 2005b).

Uncertainties in estimates of the anthropogenic component of aerosol DRF are greater than for the total aerosol, particularly over land. An uncertainty analysis (Yu et al., 2006) partitions the uncertainty for the global average anthropogenic DRF between land and ocean more or less evenly. Five parameters, namely fine-mode fraction (f_f) and anthropogenic fraction of fine-mode fraction (f_{af}) over both land and ocean, and τ over ocean, contribute nearly 80% of the overall uncertainty in the anthropogenic DRF estimate, with individual shares ranging from 13-20% (Yu et al., 2006). These uncertainties presumably represent a lower bound because the sources of error are assumed to be independent. Uncertainties associated with several parameters are also not well defined. Nevertheless, such uncertainty analysis is useful for guiding future research and documenting advances in understanding.

2.3.5. Aerosol-Cloud Interactions and Indirect Forcing

Satellite views of the Earth show a planet whose albedo is dominated by dark oceans and vegetated surfaces, white clouds, and bright deserts. The bright white clouds overlying darker oceans or vegetated surface demonstrate the significant effect that clouds have on the Earth's radiative balance. Low clouds reflect

Table 2.7. Estimates of anthropogenic components of aerosol optical depth (τ_{ant}) and clear-sky DRF at the TOA from model simulations (Schulz et al., 2006) and approaches constrained by satellite observations (Kaufman et al., 2005a; Bellouin et al., 2005, 2008; Chung et al., 2005; Yu et al., 2006; Christopher et al., 2006; Matsui and Pielke, 2006; Quaas et al., 2008; Zhao et al., 2008b).

Data Sources	Ocean		Land		Global		Estimated uncertainty or model diversity for DRF
	τ_{ant}	DRF (W m^{-2})	τ_{ant}	DRF (W m^{-2})	τ_{ant}	DRF (W m^{-2})	
Kaufman et al. (2005a)	0.033	-1.4					30%
Bellouin et al. (2005)	0.028	-0.8	0.13		0.062	-1.9	15%
Chung et al. (2005)						-1.1	
Yu et al. (2006)	0.031	-1.1	0.088	-1.8	0.048	-1.3	47% (ocean), 84% (land), and 62% (global)
Christopher et al. (2006)		-1.4					65%
Matsui and Pielke (2006)		-1.6					30°S-30°N oceans
Quaas et al. (2008)		-0.7		-1.8		-0.9	45%
Bellouin et al. (2008)	0.021	-0.6	0.107	-3.3	0.043	-1.3	Update to Bellouin et al. (2005) with MODIS Collection 5 data
Zhao et al. (2008b)		-1.25					35%
Schulz et al. (2006)	0.022	-0.59	0.065	-1.14	0.036	-0.77	30-40%; same emissions prescribed for all models

incoming sunlight back to space, acting to cool the planet, whereas high clouds can trap outgoing terrestrial radiation and act to warm the planet. In the Arctic, low clouds have also been shown to warm the surface (Garrett and Zhao, 2006). Changes in cloud cover, in cloud vertical development, and cloud optical properties will have strong radiative and therefore, climatic impacts. Furthermore, factors that change cloud development will also change precipitation processes. These changes may alter amounts, locations and intensities of local and regional rain and snowfall, creating droughts, floods and severe weather.

Cloud droplets form on a subset of aerosol particles called cloud condensation nuclei (CCN). In general, an increase in aerosol leads to an increase in CCN and an increase in drop concentration. Thus, for the same amount of liquid water in a cloud, more available CCN will result in a greater number but smaller size of droplets (Twomey, 1977). A cloud with smaller but more numerous droplets will be brighter and reflect more sunlight to space, thus exerting a cooling effect. This is the first aerosol indirect radiative effect, or "albedo effect". The effectiveness of a particle as a CCN depends on its size and composition so that the degree to which clouds become brighter for a given aerosol perturbation, and therefore the extent of cooling, depends on the aerosol size distribution and its size-dependent composition. In addition, aerosol perturbations to cloud microphysics may involve feedbacks; for example, smaller drops are less likely to collide and coalesce; this will inhibit growth, suppressing precipitation, and possibly increasing cloud lifetime (Albrecht et al., 1989). In this case clouds may exert an even stronger cooling effect.

A distinctly different aerosol effect on clouds exists in thin Arctic clouds (LWP < 25 g m^{-2}) having low emissivity. Aerosol has been shown

to increase the longwave emissivity in these clouds, thereby *warming* the surface (Lubin and Vogelman, 2006; Garrett and Zhao, 2006).

Some aerosol particles, particularly black carbon and dust, also act as ice nuclei (IN) and in so doing, modify the microphysical properties of mixed-phase and ice-clouds. An increase in IN will generate more ice crystals, which grow at the expense of water droplets due to the difference in vapor pressure over ice and water surfaces. The efficient growth of ice particles may increase the precipitation efficiency. In deep convective, polluted clouds there is a delay in the onset of freezing because droplets are smaller. These clouds may eventually precipitate, but only after higher altitudes are reached that result in taller cloud tops, more lightning and greater chance of severe weather (Rosenfeld and Lensky, 1998; Andreae et al., 2004). The present state of knowledge of the nature and abundance of IN, and ice formation in clouds is extremely poor. There is some observational evidence of aerosol influences on ice processes, but a clear link between aerosol, IN concentrations, ice crystal concentrations and growth to precipitation has not been established. This report therefore only peripherally addresses ice processes. More information can be found in a review by the WMO/IUGG International Aerosol-Precipitation Scientific Assessment (Levin and Cotton, 2008).

The present state of knowledge of the nature and abundance of ice nuclei and ice formation in clouds is extremely poor.

In addition to their roles as CCN and IN, aerosols also absorb and scatter light, and therefore they can change atmospheric conditions (temperature, stability, and surface fluxes) that influence cloud development and properties (Hansen et al., 1997; Ackerman et al., 2000). Thus, aerosols affect clouds through changing cloud droplet size distributions, cloud particle phase, and by changing the atmospheric environment of the cloud.

2.3.5a. Remote Sensing of Aerosol-Cloud Interactions and Indirect Forcing

The AVHRR satellite instruments have observed relationships between columnar aerosol loading, retrieved cloud microphysics, and cloud brightness over the Amazon Basin that are consistent with the theories explained above (Kaufman and Nakajima, 1993; Kaufman and Fraser, 1997; Feingold et al., 2001), but do not necessarily prove a causal relationship. Other studies have linked cloud and aerosol microphysical parameters or cloud albedo and droplet size using satellite data applied over the entire global oceans (Wetzel and Stowe, 1999; Nakajima et al., 2001; Han et al., 1998). Using these correlations with estimates of aerosol increase from the pre-industrial era, estimates of anthropogenic aerosol indirect radiative forcing fall into the range of -0.7 to -1.7 W m^{-2} (Nakajima et al., 2001).

Introduction of the more modern instruments (POLDER and MODIS) has allowed more detailed observations of relationships between aerosol and cloud parameters. Cloud cover can both decrease and increase with increasing aerosol loading (Koren et al., 2004; Kaufman et al., 2005c; Koren et al., 2005; Sekiguchi et al., 2003; Matheson et al., 2005; Yu et al., 2007). The same is true of LWP (Han et al., 2002; Matsui et al., 2006). Aerosol absorption appears to be an important factor in determining how cloud cover will respond to increased aerosol loading (Kaufman and Koren, 2006; Jiang and Feingold, 2006; Koren et al., 2008). Different responses of cloud cover to increased aerosol could also be correlated with atmospheric thermodynamic and moisture structure (Yu et al., 2007). Observations in the MODIS data show that aerosol loading correlates with enhanced convection and greater production of ice anvils in the summer Atlantic Ocean (Koren et al., 2005), which conflicts with previous results that used AVHRR and could not isolate convective systems from shallow clouds (Sekiguchi et al., 2003).

In recent years, surface-based remote sensing has also been applied to address aerosol effects on cloud microphysics. This method offers some interesting insights, and is complementary to the global satellite view. Surface remote sensing can only be applied at a limited number of locations, and therefore lacks the global satellite view. However, these surface stations yield high temporal resolution data and because they sample aerosol below, rather than adjacent to clouds they do not suffer from "cloud contamination". With the appropriate instrumentation (lidar) they can measure the local aerosol entering the clouds, rather than a column-integrated aerosol optical depth. Under well-mixed conditions, surface *in situ* aerosol measurements can be used. Surface remote-sensing studies are discussed in more

detail below, although the main science issues are common to satellite remote sensing.

Feingold et al. (2003) used data collected at the ARM Southern Great Plains (SGP) site to allow simultaneous retrieval of aerosol and cloud properties. A combination of a Doppler cloud radar and a microwave radiometer was used to retrieve cloud drop effective radius r_e profiles in non-precipitating (radar reflectivity Z < -17 dBZ), ice-free clouds. Simultaneously, sub-cloud aerosol extinction profiles were measured with a lidar to quantify the response of drop sizes to changes in aerosol properties. Cloud data were binned according to liquid water path (LWP) as measured with a microwave radiometer, consistent with Twomey's (1977) conceptual view of the aerosol impact on cloud microphysics. With high temporal/spatial resolution data (on the order of 20's or 100's of meters), realizations of aerosol-cloud interactions at the large eddy scale were obtained, and quantified in terms of the relative decrease in r_e in response to a relative increase in aerosol extinction ($d\ln r_e/d\ln$ extinction), as shown in Figure 2.14. Examining the dependence in this way reduces reliance on absolute measures of cloud and aerosol parameters and minimizes sensitivity to measurement error, provided errors are unbiased. This formulation permitted these responses to be related to cloud microphysical theory. Restricting the examination to updrafts only (as determined from the radar Doppler signal) permitted examination of the role of updraft in determining the response of r_e to changes in aerosol (via changes in drop number concentration N_d). Analysis of data from 7 days showed that turbulence intensifies the aerosol impact on cloud microphysics.

In addition to radar/microwave radiometer retrievals of aerosol and cloud properties, measurements of cloud optical depth by surface based radiometers such as the MFRSR (Michalsky et al., 2001) have been used in combination with measurements of cloud LWP by microwave radiometer to measure an average value of r_e during daylight when the solar elevation angle is sufficiently high (Min and Harrison, 1996). Using this retrieval, Kim et al. (2003) performed analyses of the r_e response to changes in aerosol at the same continental site, using a surface measurement of the aerosol light scattering coefficient instead of using extinction near cloud base as a proxy for CCN. Variance in LWP was shown to explain most of the variance in cloud optical depth, exacerbating detection of an aerosol effect. Although a decrease in r_e was observed with increasing scattering coefficient, the relation was not strong, indicative of other influences on r_e and/or decoupling between the surface and cloud layer. A similar study was conducted by Garrett et al. (2004) at a location in the Arctic.

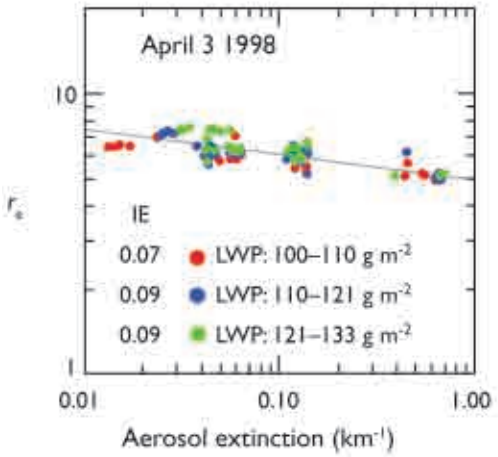

Figure 2.14. Scatter plots showing mean cloud drop effective radius (r_e) vs. aerosol extinction coefficient (unit: km^{-1}) for various liquid water path (LWP) bands on April 3, 1998 at ARM SGP site (adapted from Feingold et al., 2003).

They suggested that summertime Arctic clouds are more sensitive to aerosol perturbations than clouds at lower latitudes. The advantage of the MFRSR/microwave radiometer combination is that it derives r_e from cloud optical depth and LWP and it is not as sensitive to large drops as the radar is. A limitation is that it can be applied only to clouds with extensive horizontal cover during daylight hours.

More recent data analyses by Feingold et al. (2006), Kim et al. (2008) and McComiskey et al. (2008b) at a variety of locations, and modeling work (Feingold, 2003) have investigated (i) the use of different proxies for cloud condensation nuclei, such as the light scattering coefficient and aerosol index; (ii) sensitivity of cloud microphysical/optical properties to controlling factors such as aerosol size distribution, entrainment, LWP, and updraft velocity; (iii) the effect of optical- as opposed to radar-retrievals of drop size; and (iv) spatial heterogeneity. These studies have reinforced the importance of LWP and vertical velocity as controlling parameters. They have also begun to reconcile the reasons for the large discrepancies between various approaches, and platforms (satellite, aircraft *in situ*, and surface-based remote sensing). These investigations are important because sat-

ellite measurements that use a similar approach are being employed in GCMs to represent the albedo indirect effect (Quaas and Boucher, 2005). In fact, the weakest albedo indirect effect in IPCC (2007) derives from satellite measurements that have very weak responses of r_e to changes in aerosol. The relationship between these aerosol-cloud microphysical responses and cloud radiative forcing has been examined by McComiskey and Feingold (2008). They showed that for plane-parallel clouds, a typical uncertainty in the logarithmic gradient of a r_e-aerosol relationship of 0.05 results in a local forcing error of -3 to -10 W m^{-2}, depending on the aerosol perturbation. This sensitivity reinforces the importance of adequate quantification of aerosol effects on cloud microphysics to assessment of the radiative forcing, i.e., the indirect effect. Quantification of these effects from remote sensors is exacerbated by measurement errors. For example, LWP is measured to an accuracy of 25 g m^{-2} at best, and since it is the thinnest clouds (i.e., low LWP) that are most susceptible (from a radiative forcing perspective) to changes in aerosol, this measurement uncertainty represents a significant uncertainty in whether the observed response is related to aerosol, or to differences in LWP. The accuracy and spatial resolution of satellite-based LWP measurements is much poorer and this represents a significant challenge. In some cases important measurements are simply absent, e.g., updraft is not measured from satellite-based remote sensors.

The aerosol effect on precipitation is far more complex than the albedo effect because the instantaneous view provided by satellites makes it difficult to establish causal relationships.

Finally, cloud radar data from CloudSat, along with the A-train aerosol data, is providing great opportunity for inferring aerosol effects on precipitation (e.g., Stephens and Haynes, 2007). The aerosol effect on precipitation is far more complex than the albedo effect because the instantaneous view provided by satellites makes it difficult to establish causal relationships.

2.3.5b. In Situ Studies of Aerosol-Cloud Interactions

In situ observations of aerosol effects on cloud microphysics date back to the 1950s and 1960s (Gunn and Phillips, 1957; Squires, 1958; Warner, 1968; Warner and Twomey, 1967; Radke et al., 1989; Leaitch et al., 1992; Brenguier et al., 2000; to name a few). These studies showed that high concentrations of CCN from anthropogenic sources, such as industrial pollution or the burning of sugarcane, can increase cloud droplet number concentration N_d, thus increasing cloud microphysical stability and potentially reducing precipitation efficiency. As in the case of remote sensing studies, the causal link between aerosol perturbations and cloud microphysical responses (e.g., r_e or N_d) is much better established than the relationship between aerosol and changes in cloud fraction, LWC, and precipitation (see also Levin and Cotton, 2008).

In situ cloud measurements are usually regarded as "ground truth" for satellite retrievals but in fact there is considerable uncertainty in measured parameters such liquid water content (LWC), and size distribution, which forms the basis of other calculations such as drop concentration, r_e and extinction. It is not uncommon to see discrepancies in LWC on the order of 50% between different instruments, and cloud drop size distributions are difficult to measure, particularly for droplets < 10 μm where Mie scattering oscillations generate ambiguities in drop size. Measurement uncertainty in r_e from *in situ* probes is assessed, for horizontally homogeneous clouds, to be on the order of 15-20%, compared to 10% for MODIS and 15-20% for other spectral measurements (Feingold et al., 2006). As with remote measurements it is prudent to consider relative (as opposed to absolute) changes in cloud microphysics related to relative changes in aerosol. An added consideration is that *in situ* measurements typically represent a very small sample of the atmosphere akin to a thin pencil line through a large volume. For an aircraft flying at 100 m s^{-1} and sampling at 1 Hz, the sample volume is on the order of 10 cm^3. The larger spatial sampling of remote sensing has the advantage of being more representative but it removes small-scale (i.e., sub sampling-volume) variability, and therefore may obscure important cloud processes.

Measurements at a wide variety of locations around the world have shown that increases in aerosol concentration lead to increases in N_d. However the rate of this increase is highly variable and always sub-linear, as exemplified by the compilation of data in Ramanathan et al. (2001a). This is because, as discussed previously, N_d is a function of numerous parameters in addition to aerosol number concentration, including size distribution, updraft veloc-

ity (Leaitch et al., 1996), and composition. In stratocumulus clouds, characterized by relatively low vertical velocity (and low supersaturation) only a small fraction of particles can be activated whereas in vigorous cumulus clouds that have high updraft velocities, a much larger fraction of aerosol particles is activated. Thus the ratio of N_d to aerosol particle number concentration is highly variable.

In recent years there has been a concerted effort to reconcile measured N_d concentrations with those calculated based on observed aerosol size and composition, as well as updraft velocity. These so-called "closure experiments" have demonstrated that on average, agreement in N_d between these approaches is on the order of 20% (e.g., Conant et al., 2004). This provides confidence in theoretical understanding of droplet activation, however, measurement accuracy is not high enough to constrain the aerosol composition effects that have magnitudes < 20%.

One exception to the rule that more aerosol particles result in larger N_d is the case of giant CCN (sizes on the order of a few microns), which, in concentrations on the order of 1 cm^{-3} (i.e., ~ 1% of the total concentration) can lead to significant suppression in cloud supersaturation and reductions in N_d (O'Dowd et al., 1999). The measurement of these large particles is difficult and hence the importance of this effect is hard to assess. These same giant CCN, at concentrations as low as 1/liter, can significantly affect the initiation of precipitation in moderately polluted clouds (Johnson, 1982) and in so doing alter cloud albedo (Feingold et al., 1999).

The most direct link between the remote sensing of aerosol-cloud interactions discussed in section 2.3.5.1 and *in situ* observations is via observations of relationships between drop concentration N_d and CCN concentration. Theory shows that if r_e-CCN relationships are calculated at constant LWP or LWC, their logarithmic slope is -1/3 that of the N_d-CCN logarithmic slope (i.e., $d\ln r_e/d\ln CCN = -1/3\, d\ln N_d/d\ln CCN$). In general, N_d-CCN slopes measured *in situ* tend to be stronger than equivalent slopes obtained from remote sensing – particularly in the case of satellite remote sensing (McComiskey and Feingold 2008). There are a number of reasons for this: (i) *in situ* measurements focus on smaller spatial scales and are more likely to observe the droplet activation process as opposed to remote sensing that incorporates larger spatial scales and includes other processes such as drop coalescence that reduce N_d, and therefore the slope of the N_d-CCN relationship (McComiskey et al., 2008b). (ii) Satellite remote sensing studies typically do not sort their data by LWP, and this has been shown to reduce the magnitude of the r_e-CCN response (Feingold, 2003).

In conclusion, observational estimates of aerosol indirect radiative forcings are still in their infancy. Effects on cloud microphysics that result in cloud brightening have to be considered along with effects on cloud lifetime, cover, vertical development and ice production. For *in situ* measurements, aerosol effects on cloud microphysics are reasonably consistent (within ~ 20%) with theory but measurement uncertainties in remote sensing of aerosol effects on clouds, as well as complexity associated with three-dimensional radiative transfer, result in considerable uncertainty in radiative forcing. The higher order indirect effects are poorly understood and even the sign of the microphysical response and forcing may not always be the same. Aerosol type and specifically the absorption properties of the aerosol may cause different cloud responses. Early estimates of observationally based aerosol indirect forcing range from -0.7 to -1.7 W m^{-2} (Nakajima et al., 2001) and -0.6 to -1.2 W m^{-2} (Sekiguchi et al., 2003), depending on the estimate for aerosol increase from pre-industrial times and whether aerosol effects on cloud fraction are also included in the estimate.

For *in situ* measurements, aerosol effects on cloud microphysics are reasonably consistent with theory but measurement uncertainties in remote sensing of aerosol effects on clouds result in considerable uncertainty in radiative forcing.

2.4. Outstanding Issues

Despite substantial progress, as summarized in section 2.2 and 2.3, most measurement-based studies so far have concentrated on influences produced by the sum of natural and anthropogenic aerosols on solar radiation under clear sky conditions. Important issues remain:

- Because accurate measurements of aerosol absorption are lacking and land surface reflection values are uncertain, DRF estimates over land and at the ocean surface are less well constrained than the estimate of TOA DRF over ocean.
- Current estimates of the anthropogenic component of aerosol direct radiative forcing have large uncertainties, especially over land.

- Because there are very few measurements of aerosol absorption vertical distribution, mainly from aircraft during field campaigns, estimates of direct radiative forcing of above-cloud aerosols and profiles of atmospheric radiative heating induced by aerosol absorption are poorly constrained.
- There is a need to quantify aerosol impacts on thermal infrared radiation, especially for dust.
- The diurnal cycle of aerosol direct radiative forcing cannot be adequately characterized with currently available, sun-synchronous, polar orbiting satellite measurements.
- Measuring aerosol, cloud, and ambient meteorology contributions to indirect radiative forcing remains a major challenge.
- Long-term aerosol trends and their relationship to observed surface solar radiation changes are not well understood.

There is a need to pursue a better understanding of the uncertainty in single scattering albedo from both *in situ* measurements and remote sensing retrievals.

The current status and prospects for these areas are briefly discussed below.

Measuring aerosol absorption and single-scattering albedo: Currently, the accuracy of both *in situ* and remote sensing aerosol SSA measurements is generally ±0.03 at best, which implies that the inferred accuracy of clear sky aerosol DRF would be larger than 1 W m^{-2} (see Chapter 1). Recently developed photoacoustic (Arnott et al., 1997) and cavity ring down extinction cell (Strawa et al., 2002) techniques for measuring aerosol absorption produce SSA with improved accuracy over previous methods. However, these methods are still experimental, and must be deployed on aircraft. Aerosol absorption retrievals from satellites using the UV-technique have large uncertainties associated with its sensitivity to the height of the aerosol layer(s) (Torres et al., 2005), and it is unclear how the UV results can be extended to visible wavelengths. Views in and out of sunglint can be used to retrieve total aerosol extinction and scattering, respectively, thus constraining aerosol absorption over oceans (Kaufman et al., 2002b). However, this technique requires retrievals of aerosol scattering properties, including the real part of the refractive index, well beyond what has so far been demonstrated from space. In summary, there is a need to pursue a better understanding of the uncertainty in SSA from both *in situ* measurements and remote sensing retrievals and, with this knowledge, to synthesize different data sets to yield a characterization of aerosol absorption with well-defined uncertainty (Leahy et al., 2007). Laboratory studies of aerosol absorption of specific known composition are also needed to interpret *in situ* measurements and remote sensing retrievals and to provide updated database of particle absorbing properties for models.

Estimating the aerosol direct radiative forcing over land: Land surface reflection is large, heterogeneous, and anisotropic, which complicates aerosol retrievals and DRF determination from satellites. Currently, the aerosol retrievals over land have relatively lower accuracy than those over ocean (Section 2.2.5) and satellite data are rarely used alone for estimating DRF over land (Section 2.3). Several issues need to be addressed, such as developing appropriate angular models for aerosols over land (Patadia et al., 2008) and improving land surface reflectance characterization. MODIS and MISR measure land surface reflection wavelength dependence and angular distribution at high resolution (Moody et al., 2005; Martonchik et al., 1998b; 2002). This offers a promising opportunity for inferring the aerosol direct radiative forcing over land from satellite measurements of radiative fluxes (e.g., CERES) and from critical reflectance techniques (Fraser and Kaufman, 1985; Kaufman, 1987). The aerosol direct radiative forcing over land depends strongly on aerosol absorption and improved measurements of aerosol absorption are required.

Distinguishing anthropogenic from natural aerosols: Current estimates of anthropogenic components of AOD and direct radiative forcing have larger uncertainties than total aerosol optical depth and direct radiative forcing, particularly over land (see Section 2.3.4), because of relatively large uncertainties in the retrieved aerosol microphysical properties (see Section 2.2). Future measurements should focus on improved retrievals of such aerosol properties as size distribution, particle shape, and absorption, along with algorithm refinement for better aerosol optical depth retrievals. Coordinated *in situ* measurements offer a promising avenue for validating and refining satellite identification of anthropogenic aerosols (Anderson et al., 2005a, 2005b). For satellite-based aerosol type characterization, it is sometimes assumed that

all biomass-burning aerosol is anthropogenic and all dust aerosol is natural (Kaufman et al., 2005a). The better determination of anthropogenic aerosols requires a quantification of biomass burning ignited by lightning (natural origin) and mineral dust due to human induced changes of land cover/land use and climate (anthropogenic origin). Improved emissions inventories and better integration of satellite observations with models seem likely to reduce the uncertainties in aerosol source attribution.

Profiling the vertical distributions of aerosols: Current aerosol profile data are far from adequate for quantifying the aerosol radiative forcing and atmospheric response to the forcing. The data have limited spatial and temporal coverage, even for current spaceborne lidar measurements. Retrieving aerosol extinction profile from lidar measured attenuated backscatter is subject to large uncertainties resulting from aerosol type characterization. Current space-borne Lidar measurements are also not sensitive to aerosol absorption. Because of lack of aerosol vertical distribution observations, the estimates of DRF in cloudy conditions and dust DRF in the thermal infrared remain highly uncertain (Schulz et al., 2006; Sokolik et al., 2001; Lubin et al., 2002). It also remains challenging to constrain the aerosol-induced atmospheric heating rate increment that is essential for assessing atmospheric responses to the aerosol radiative forcing (e.g., Yu et al., 2002; Feingold et al., 2005; Lau et al., 2006). Progress in the foreseeable future is likely to come from (1) better use of existing, global, space-based backscatter lidar data to constrain model simulations, and (2) deployment of new instruments, such as high-spectral-resolution lidar (HSRL), capable of retrieving both extinction and backscatter from space. The HSRL lidar system will be deployed on the EarthCARE satellite mission tentatively scheduled for 2013 (http://asimov/esrin.esi.it/esaLP/ASESMYNW9SC_Lpearthcare_1.html).

Characterizing the diurnal cycle of aerosol direct radiative forcing: The diurnal variability of aerosol can be large, depending on location and aerosol type (Smirnov et al., 2002), especially in wildfire situations, and in places where boundary layer aerosols hydrate or otherwise change significantly during the day. This cannot be captured by currently available, sun-synchronous, polar orbiting satellites. Geostationary satellites provide adequate time resolution (Christopher and Zhang, 2002; Wang et al., 2003), but lack the information required to characterize aerosol types. Aerosol type information from low earth orbit satellites can help improve accuracy of geostationary satellite aerosol retrievals (Costa et al., 2004a, 2004b). For estimating the diurnal cycle of aerosol DRF, additional efforts are needed to adequately characterize the anisotropy of surface reflection (Yu et al., 2004) and daytime variation of clouds.

Studying aerosol-cloud interactions and indirect radiative forcing: Remote sensing estimates of aerosol indirect forcing are still rare and uncertain. Improvements are needed for both aerosol characterization and measurements of cloud properties, precipitation, water vapor, and temperature profiles. Basic processes still need to be understood on regional and global scales. Remote sensing observations of aerosol-cloud interactions and aerosol indirect forcing are for the most part based on simple correlations among variables, from which cause-and-effects cannot be deduced. One difficulty in inferring aerosol effects on clouds from the observed relationships is separating aerosol from meteorological effects, as aerosol loading itself is often correlated with the meteorology. In addition, there are systematic errors and biases in satellite aerosol retrievals for partly cloud-filled scenes. Stratifying aerosol and cloud data by liquid water content, a key step in quantifying the albedo (or first) indirect effect, is usually missing. Future work will need to combine satellite observations with *in situ* validation and modeling interpretation. A methodology for integrating observations (*in situ* and remote) and models at the range of relevant temporal/spatial scales is crucial to improve understanding of aerosol indirect effects and aerosol-cloud interactions.

Remote sensing estimates of aerosol indirect forcing are still rare and uncertain. Improvements are needed for both aerosol characterization and measurements of cloud properties, precipitation, water vapor, and temperature profiles.

Quantifying long-term trends of aerosols at regional scales: Because secular changes are subtle, and are superposed on seasonal and other natural variability, this requires the construction of consistent, multi-decadal records of climate-quality data. To be meaningful, aerosol trend analysis must be performed on a regional basis. Long-term trends of aerosol optical depth have been studied using measurements from surface remote sensing stations (e.g., Hoyt and

To be meaningful, aerosol trend analysis must be performed on a regional basis.

Frohlich, 1983; Augustine et al., 2008; Luo et al., 2001) and historic satellite sensors (Massie et al., 2004; Mishchenko et al., 2007a; Mishchenko and Geogdzhayev, 2007; Zhao et al., 2008a). An emerging multi-year climatology of high quality AOD data from modern satellite sensors (e.g., Remer et al., 2008; Kahn et al., 2005a) has been used to examine the inter-annual variations of aerosol (e.g., Koren et al., 2007a, Mishchenko and Geogdzhayev, 2007) and contribute significantly to the study of aerosol trends. Current observational capability needs to be continued to avoid any data gaps. A synergy of aerosol products from historical, modern and future sensors is needed to construct as long a record as possible. Such a data synergy can build upon understanding and reconciliation of AOD differences among different sensors or platforms (Jeong et al., 2005). This requires overlapping data records for multiple sensors. A close examination of relevant issues associated with individual sensors is urgently needed, including sensor calibration, algorithm assumptions, cloud screening, data sampling and aggregation, among others.

A better understanding of aerosol-radiation-cloud interactions and trends in cloudiness, cloud albedo, and surface albedo is badly needed to attribute the observed radiation changes to aerosol changes with less ambiguity.

Linking aerosol long-term trends with changes of surface solar radiation: Analysis of the long-term surface solar radiation record suggests significant trends during past decades (e.g., Stanhill and Cohen, 2001; Wild et al., 2005; Pinker et al., 2005; Alpert et al., 2005). Although a significant and widespread decline in surface total solar radiation (the sum of direct and diffuse irradiance) occurred up to 1990 (so-called solar dimming), a sustained increase has been observed during the subsequent decade. Speculation suggests that such trends result from decadal changes of aerosols and the interplay of aerosol direct and indirect radiative forcing (Stanhill and Cohen, 2001; Wild et al., 2005; Streets et al., 2006a; Norris and Wild, 2007; Ruckstuhl et al., 2008). However, reliable observations of aerosol trends are required test these ideas. In addition to aerosol optical depth, changes in aerosol composition must also be quantified, to account for changing industrial practices, environmental regulations, and biomass burning emissions (Novakov et al., 2003; Streets et al., 2004; Streets and Aunan et al., 2005). Such compositional changes will affect the aerosol SSA and size distribution, which in turn will affect the surface solar radiation (e.g., Qian et al., 2007). However such data are currently rare and subject to large uncertainties. Finally, a better understanding of aerosol-radiation-cloud interactions and trends in cloudiness, cloud albedo, and surface albedo is badly needed to attribute the observed radiation changes to aerosol changes with less ambiguity.

2.5. Concluding Remarks

Since the concept of aerosol-radiation-climate interactions was first proposed around 1970, substantial progress has been made in determining the mechanisms and magnitudes of these interactions, particularly in the last ten years. Such progress has greatly benefited from significant improvements in aerosol measurements and increasing sophistication of model simulations. As a result, knowledge of aerosol properties and their interaction with solar radiation on regional and global scales is much improved. Such progress plays a unique role in the definitive assessment of the global anthropogenic radiative forcing, as *"virtually certainly positive"* in IPCC AR4 (Haywood and Schulz, 2007).

***In situ* measurements of aerosols:** New *in situ* instruments such as aerosol mass spectrometers, photoacoustic techniques, and cavity ring down cells provide high accuracy and fast time resolution measurements of aerosol chemical and optical properties. Numerous focused field campaigns and the emerging ground-based aerosol networks are improving regional aerosol chemical, microphysical, and radiative property characterization. Aerosol closure studies of different measurements indicate that measurements of submicrometer, spherical sulfate and carbonaceous particles have a much better accuracy than that for dust-dominated aerosol. The accumulated comprehensive data sets of regional aerosol properties provide a rigorous "test bed" and strong constraint for satellite retrievals and model simulations of aerosols and their direct radiative forcing.

Remote sensing measurements of aerosols: Surface networks, covering various aerosol regimes around the globe, have been measuring aerosol optical depth with an accuracy of 0.01~0.02, which is adequate for achieving the accuracy of 1 W m^{-2} for cloud-free TOA DRF. On the other hand, aerosol microphysical properties retrieved from these networks, especially

SSA, have relatively large uncertainties and are only available in very limited conditions. Current satellite sensors can measure AOD with an accuracy of about 0.05 or 15 to 20% in most cases. The implementation of multi-wavelength, multi-angle, and polarization measuring capabilities has also made it possible to measure particle properties (size, shape, and absorption) that are essential for characterizing aerosol type and estimating anthropogenic component of aerosols. However, these microphysical measurements are more uncertain than AOD measurements.

Observational estimates of clear-sky aerosol direct radiative forcing: Closure studies based on focused field experiments reveal DRF uncertainties of about 25% for sulfate/carbonaceous aerosol and 60% for dust at regional scales. The high-accuracy of MODIS, MISR and POLDER aerosol products and broadband flux measurements from CERES make it feasible to obtain observational constraints for aerosol TOA DRF at a global scale, with relaxed requirements for measuring particle microphysical properties. Major conclusions from the assessment are:

- A number of satellite-based approaches consistently estimate the clear-sky diurnally averaged TOA DRF (on solar radiation) to be about -5.5±0.2 W m^{-2} (mean ± standard error from various methods) over global ocean. At the ocean surface, the diurnally averaged DRF is estimated to be -8.7±0.7 W m^{-2}. These values are calculated for the difference between today's measured total aerosol (natural plus anthropogenic) and the absence of all aerosol.
- Overall, in comparison to that over ocean, the DRF estimates over land are more poorly constrained by observations and have larger uncertainties. A few satellite retrieval and satellite-model integration yield the over-land clear-sky diurnally averaged DRF of -4.9±0.7 W m^{-2} and -11.8±1.9 W m^{-2} at the TOA and surface, respectively. These values over land are calculated for the difference between total aerosol and the complete absence of all aerosol.
- Use of satellite measurements of aerosol microphysical properties yields that on a global ocean average, about 20% of AOD is contributed by human activities and the clear-sky TOA DRF by anthropogenic aerosols is -1.1±0.4 W m^{-2}. Similar DRF estimates are rare over land, but a few measurement-model integrated studies do suggest much more negative DRF over land than over ocean.
- These satellite-based DRF estimates are much greater than the model-based estimates, with differences much larger at regional scales than at a global scale.

Measurements of aerosol-cloud interactions and indirect radiative forcing: *In situ* measurement of cloud properties and aerosol effects on cloud microphysics suggest that theoretical understanding of the activation process for water cloud is reasonably well-understood. Remote sensing of aerosol effects on droplet size associated with the albedo effect tends to underestimate the magnitude of the response compared to *in situ* measurements. Recent efforts trace this to a combination of lack of stratification of data by cloud water, the relatively large spatial scale over which measurements are averaged (which includes variability in cloud fields, and processes that obscure the aerosol-cloud processes), as well as measurement uncertainties (particularly in broken cloud fields). It remains a major challenge to infer aerosol number concentrations from satellite measurements. The present state of knowledge of the nature and abundance of IN, and ice formation in clouds is extremely poor.

The high-accuracy of satellite measurements makes it feasible to obtain observational constraints for aerosol top-of-atmosphere direct radiative forcing at a global scale.

Despite the substantial progress in recent decades, several important issues remain, such as measurements of aerosol size distribution, particle shape, absorption, and vertical profiles, and the detection of aerosol long-term trend and establishment of its connection with the observed trends of solar radiation reaching the surface, as discussed in section 2.4. Furthering the understanding of aerosol impacts on climate requires a coordinated research strategy to improve the measurement accuracy and use the measurements to validate and effectively constrain model simulations. Concepts of future research in measurements are discussed in Chapter 4 "Way Forward".

Furthering the understanding of aerosol impacts on climate requires a coordinated research strategy to improve the measurement accuracy and to constrain/validate models with measurements.

Sampling the Arcic Haze. Pollution and smoke aerosols can travel long distances, from mid-latitudes to the Arctic, causing "Arctic Haze". Photo taken from the NASA DC-8 aircraft during the ARCTAS field experiment over Alaska in April 2008. Credit: Mian Chin, NASA.